frontiers in Marine Science

ORIGINAL RESEARCH
published: 15 June 2018
doi: 10.3389/fmars.2018.00210

# Effect of Organic Fe-Ligands, Released by *Emiliania huxleyi,* on Fe(II) Oxidation Rate in Seawater Under Simulated Ocean Acidification Conditions: A Modeling Approach

*Guillermo Samperio-Ramos, J. Magdalena Santana-Casiano* and Melchor González-Dávila*

*Instituto de Oceanografía y Cambio Global (IOCAG), Universidad de Las Palmas de Gran Canaria, Las Palmas de Gran Canaria, Spain*

OPEN ACCESS

**Edited by:**
*Christopher Edward Cornwall, Victoria University of Wellington, New Zealand*

**Reviewed by:**
*Evelyn Armstrong, University of Otago, New Zealand*
*Linn Hoffmann, University of Otago, New Zealand*
*Julian Gallego Urrea, University of Gothenburg, Sweden*

***Correspondence:**
*J. Magdalena Santana-Casiano*
*magdalena.santana@ulpgc.es*

**Specialty section:**
*This article was submitted to Global Change and the Future Ocean, a section of the journal Frontiers in Marine Science*

**Received:** *04 February 2018*
**Accepted:** *29 May 2018*
**Published:** *15 June 2018*

**Citation:**
*Samperio-Ramos G, Santana-Casiano JM and González-Dávila M (2018) Effect of Organic Fe-Ligands, Released by Emiliania huxleyi, on Fe(II) Oxidation Rate in Seawater Under Simulated Ocean Acidification Conditions: A Modeling Approach. Front. Mar. Sci. 5:210. doi: 10.3389/fmars.2018.00210*

The potential effect of ocean acidification on the exudation of organic matter by phytoplankton and, consequently, on the iron redox chemistry is largely unknown. In this study, the coccolithophorid *Emiliania huxleyi* was exposed to different $pCO_2$ conditions (225–900 μatm), in order to determine the role of natural organic ligands on the Fe(II) oxidation rate. Oxidation kinetics of Fe(II) were studied as a function of pH (7.75–8.25) and dissolved organic carbon levels produced (0–141.11 μmol C $L^{-1}$) during the different growth stages. The Fe(II) oxidation rate always decreased in the presence of exudates as compared to that in the exudates-free seawater. The organic ligands present in the coccolithophorid exudates were responsible for this decrease. The oxidation of Fe(II) in artificial seawater was also investigated at nanomolar levels over a range of pH (7.75–8.25) at 25°C in the presence of different glucuronic acid concentrations. Dissolved uronic acids (DUA) slightly increased the experimental rate compared to control artificial seawater (ASW) which can be ascribed to the stabilization of the oxidized form by chelation. This behavior was a function of the Fe(II):DUA ratio and was a pH dependent process. A kinetic model in ASW, with a single organic ligand, was applied for computing the equilibrium constant (log $K_{FeCHO+} = 3.68 \pm 0.81$ $M^{-1}$) and the oxidation rate (log $k_{FeCHO+} = 3.28 \pm 0.41$ $M^{-1}$ $min^{-1}$) for the Fe(II)-DUA complex ($FeCHO^+$), providing an excellent description of data obtained over a wide range of DUA concentrations and pH conditions. Considering the Marcus theory the Fe(III) complexing constant with DUA was limited to between $10^{13}$ and $10^{16}$. For the seawater enriched with exudates of *E. huxleyi* a second kinetic modeling approach was carried out for fitting the Fe(II) speciation, and the contribution of each Fe(II) species to the overall oxidation rate as a function of the pH/$pCO_2$ conditions. The influence of organic ligands in the Fe(II) speciation diminished as pH decreased in solution. During the stationary growth phase, the $FeCHO^+$ complex became the most important contributor to the overall oxidation rate when pH was lower than 7.95. Because $CO_2$ levels modify the composition of excreted organic ligands, the redox behavior of Fe in solution may be affected by future acidification conditions.

**Keywords: *Emiliania huxleyi*, ocean acidification, Fe(II) oxidation, exudates, uronic acids, organic ligands, redox behavior, pH**

## INTRODUCTION

Iron is an essential micronutrient required for important phytoplankton physiological processes, such as nutrient assimilation and electron transport during respiration and photosynthesis (Behrenfeld and Milligan, 2013). The biological demand of iron in the ocean is conditioned by Fe-low solubility and Fe redox behavior (Shaked and Lis, 2012; Tagliabue et al., 2017). In oxygen rich waters, inorganic Fe(II) is oxidized to the thermodynamically stable ferric forms (González-Dávila et al., 2006), which are highly insoluble and precipitate as stable minerals or through scavenging onto sinking particles (Boyd and Ellwood, 2010). Nevertheless, dissolved iron in seawater is organically complexed by colloidal material or truly soluble ligands which systematically increases iron solubility (Boye et al., 2010; Caprara et al., 2016). Microbial exudates contribute appreciably to this pool of iron ligands, which have been categorized into two types ($L_1$ and $L_2$) according to their binding affinities. While evidence proposes siderophores, produced by some prokaryotes, as the main constituents of $L_1$ class ligands on the basis of their iron complexing capacities (Gledhill and Buck, 2012), the conditional stability constants of intracellular metabolic components, such as porphyrins, are similar to those of $L_2$ type ligands (Hogle et al., 2014). However, the overlapping analytical range of the competitive ligand exchange technique suggests that there may be additional weaker ligand classes present in marine systems (Bundy et al., 2014) and, therefore, their importance for iron biogeochemistry might likely be underestimated. Although exudates from bacteria and phytoplankton are not well characterized, sources of these biologically-mediated weak ligands include mainly exo-polymeric substances (EPS), since they form a major biological component of the total dissolved organic carbon (DOC) pool (Pakulski and Benner, 1994). EPS are polymers of high molecular weight mostly comprised of amino acids and saccharides (Strmečki et al., 2010; Decho and Gutierrez, 2017). As a functional group of some peptides, thiol moieties play an important role in controlling the speciation of some trace metals (Vasconcelos et al., 2002). Nevertheless, using Fourier transform infrared spectrum analysis of EPS, Ozturk et al. (2014) determined that the carboxylic groups of uronic acids confer the negative net charge of the polymer that serves both to bind metallic cations and to form resilient linkages between the polymer chains. In fact, surface active saccharides, such as uronic acids, also play a key role in oceanic carbon cycling, through coagulation and aggregation processes, by acting as precursors for transparent exopolymer particles (Passow, 2002) and representing an abiotic linkage between dissolved and particulate phases of organic carbon (Engel et al., 2004; Verdugo et al., 2004).

Microbial rich-uronic acids exudates are excreted in response to environmental stress, such as nutrient limitation (Borchard and Engel, 2012), thermal, pH and salinity variations (Lidbury et al., 2012; Underwood et al., 2013), or the presence of heavy and toxic metal ions (Gupta and Diwan, 2017). Dissolved uronic acids (DUA) can reach micromolar levels in sea surface waters, and therefore, they are an important component of the reactive organic carbon in the ocean, making up to 6% of the DOC (Khodse et al., 2010), and up to 17 and 40% of total and high-molecular-weight dissolved ($<0.45\,\mu m$) carbohydrates, respectively (Hung et al., 2001; Engel et al., 2012). Although pH-titrations indicate that the stability constants for Fe-saccharide complexes are significantly lower than for $L_1$ and $L_2$ (Gledhill and Buck, 2012), experimental evidence has indicated that sugar acids may contribute to the marine Fe ligand pool (Benner, 2011). Accordingly, the presence of DUA, as free form or as part of macromolecules, might represent an important factor to control the bioavailability of Fe in the ocean (Hassler et al., 2011; Lis et al., 2015). However, given that Fe(II) species are the most easily assimilated by phytoplankton (Shaked and Lis, 2012), the Fe-redox transformations are of crucial importance in determining the chemical form and the subsequent bioavailability of iron.

The presence of DUA in seawater can modify the Fe(II)/Fe(III)-redox balance (Kuma et al., 1995; Norman et al., 2015). However, relatively little is known about the role played by uronic acids on iron redox chemistry under different pH conditions. The presence of –COOH functional groups in sugar acids suggest that iron complexation by uronic acids can be affected by variations in pH (Millero et al., 2009). Accordingly, due to the rising anthropogenic atmospheric $CO_2$ and the consequent $CO_2$-uptake by the oceans, a shift in the carbonate chemistry system is expected (Hoegh-Guldberg and Poloczanska, 2017), as well as an important decrease in sea surface water pH from its current value of 8.1–7.8 (IPCC, 2014). Therefore this process, termed ocean acidification, may have a strong impact both on the speciation and redox behavior of iron in seawater (Hoffmann et al., 2012; Hutchins and Boyd, 2016).

Constraining the pH-dependence of Fe redox kinetics in seawater has been the goal of a number of studies over the past three decades (Moffett and Zika, 1987; Miller et al., 1995; King and Farlow, 2000; González-Dávila et al., 2006; González et al., 2016). Nevertheless, few studies have addressed this research (i.e., pH-dependence) while taking account the role played by the natural exudates produced by phytoplankton on iron redox transformations (Santana-Casiano et al., 2014). The experimental and modeled data obtained by these studies have explained the pH effect on the Fe redox chemistry in the presence of organic ligands released by the diatom *Dunaliella tertiolecta* (González et al., 2014) and the cyanobacteria *Synechococcus* PCC 7002; (Samperio-Ramos et al., 2018). Those exudates were produced and excreted at natural seawater pH and then exposed under different physicochemical conditions (González et al., 2014; Samperio-Ramos et al., 2018). However, ocean acidification might change the type and amount of dissolved organic material released by phytoplankton (Spilling et al., 2016), since pH/$pCO_2$ seawater conditions regulate the inorganic carbon concentrating mechanisms and the photosynthetic carbon fixation rates in autotrophic microorganism (Riebesell et al., 2007).

With a widely adaptive capacity, the coccolithophorid *Emiliania huxleyi* is globally distributed, ranging from equatorial to subarctic regions where it is the major large-scale bloom forming species (Read et al., 2013). These microalgae are an essential component of the carbon cycle, since they are responsible for a large part of the carbonate production in the

surface ocean (Beaufort et al., 2011) and, therefore, are highly sensitive to variations in pH/$pCO_2$ seawater conditions (Riebesell et al., 2000). Additionally, ocean acidification seems to increase the extracellular release rate of Fe organic ligands, including sugar acids, by *E. huxleyi* (Fukuda et al., 2014; Jin et al., 2015). In fact, the content of uronic acids in the coccolithophorid surface regulates crystal nucleation during calcification (Giuffre et al., 2013) and reports on the adaptation of these microalgae to $CO_2$ changes (Lee et al., 2016).

The aim of this study is to analyze the effect of organic ligands released by *E. huxleyi* on the Fe(II) oxidation rate at nanomolar levels, as a function of the concentration of DOC exuded ($DOC_E$) during different growth stages and under different $CO_2$ conditions. We also examined the oxidation kinetics of Fe(II)-DUA complexes in artificial seawater (ASW), as a function of pH and ligand concentration, in order to elucidate the influence of the uronic acids on the Fe(II) oxidation rate, in the presence of the exudates produced by *E.huxleyi*. A kinetic model (Santana-Casiano et al., 2005) was extended in order to determine the contribution and speciation of the individual ferrous species on the oxidation process, including the effect of the organic ligands exuded by *E. huxleyi,* over a wide range of scenarios of acidification in the upper ocean. More specifically, the theory of Marcus was successfully applied to the oxidation rates of Fe(II)-organic complexes (Rose and Waite, 2003), to determine if an outer-sphere electron transfer mechanism was produced during the oxygenation of Fe(II).

# MATERIALS AND METHODS

## Experimental Media and Organic Exudate Enrichment

Four experimental scenarios, based on the Intergovernmental Panel on Climate Change projections (IPCC, 2014) were fixed: interglacial, close to contemporary and two future ocean acidification conditions with $pCO_2$ 225, 350, 600, and 900 μatm respectively. Consequently, the aeration with $CO_2$-air-mixture generated constant pH values of 8.25, 8.10, 7.90, and 7.75 in the seawater where *E. huxleyi* was inoculated. A more detailed description of the experimental medium conditions and the set-up to manipulate the carbonate chemistry system are given by Samperio-Ramos et al. (2017).

Axenic cultures of *E. huxleyi* (strain RCC1238) were supplied by the Spanish Bank of Algae (BEA) in f/2 medium. The microcosms were kept in a clean culture chamber (Friocell FC111) at constant temperature (25°C), and illumination (complete photoperiod of 24 h and 200 μmol photons $m^{-2}$ of light intensity). The experimental batch cultures were inoculated in autoclaved 2.5 L polycarbonate cylindrical tanks, fitting the stock culture $CO_2$ conditions. The coccolithophorids grew in sterile-filtered (Nucleopore, 0.1 μm) North Atlantic seawater, obtained at the ESTOC site (29° 10′ N, 15° 30′ W) at 250 m depth and enriched (SWEN) with sodium nitrate (Sigma-Aldrich), potassium hydrogen phosphate (Sigma-Aldrich) and sodium metasilicate (Sigma-Aldrich) (850, 25, and 140 μM respectively). The salinity (36.48 ± 0.001) was measured with a salinometer (Portasal 8410A). To ensure both gas homogeneity and cell suspension in the solution, the cultures were gently stirred (60 rpm) with Teflon-coated magnetic bars [(Sachs and Kawka, 2015)]. The stock and experimental cultures were tested weekly for bacterial contamination and cell damage.

The growth curves of *E. huxleyi* (Samperio-Ramos et al., 2017), under the different $CO_2$ scenarios, followed a sigmoidal behavior, showing a lag phase (LP: 1st−3rd day of culture), an exponential phase (EP: 4th−6th) and a stationary phase (SP: after 7th day). Different prior incubation times, for the adaptation to $CO_2$ simulated conditions, can change the metabolic response of microorganisms (Hurd et al., 2009). Thus, in order to minimize and standardize possible physiological responses, the stock cultures were considered acclimated to the pH conditions when in the mesocosms no significant differences were found between the growth rates given during the EP, after several consecutive transfers. The selected aliquots from *E. huxleyi* stock cultures were centrifuged 3 times (600 × g for 15 min at 15°C) with SWEN to avoid introducing chemical buffers from the f/2 medium, which might interact with iron during the kinetic experiments (Santana-Casiano et al., 2000) or cause changes in the trace metal bioavailability during batch cultures (Shi et al., 2010). Once the cultures were filtered (0.45 μm), the seawater enriched with organic exudates (SWEX) was used to carry out the organic assays and the Fe(II) oxidation kinetic studies. Equipment in contact with SWEN, culturing solutions and ASW was cleaned for trace metals according to a standard protocol (Achterberg et al., 2001).

## Organic Determination

$DOC_E$ concentration in cultures was monitored by the high temperature oxidation method using a Total Organic Carbon analyzer (Shimadzu TOC-V), previously calibrated from standard curves (20–300 μmol C $L^{-1}$) with potassium hydrogen phthalate (Sigma-Aldrich) (Arístegui et al., 2014). DOC reference material (Dr. Hansell; University of Miami) was analyzed to check the accuracy and precision. The coefficient of variation of the method was <3%. The measures of certified reference material had a standard deviation of 0.99 μmol C $L^{-1}$. The instrument blank (3–10 μmol C $L^{-1}$) was measured using UV-irradiated Milli-Q water and was subtracted from each sample.

In order to have a measurable level of exuded DUA ($DUA_E$), the samples were concentrated by rotary evaporation, under reduced pressure at 40°C. Then, the concentrations of DUA were measured according to the method reported by Bastos et al. (2015). Thus, 3 mL of 75 mM sodium tetraborate (Sigma-Aldrich), prepared in sulfuric acid (1 M), was added to 0.5 mL of concentrate sample. The resulting solution was heated at 100°C for 10 min in a boiling water bath. After cooling, 100 μL 0.15% m-hydroxydiphenyl (Sigma-Aldrich) was added, and the absorbance determined spectrophotometrically at 525 nm. The reagent blank was subtracted in order to compute the final concentration of monosaccharides. Galacturonic acid (Sigma-Aldrich) was used as a standard. The method had an uncertainty of 5%.

The units of $DOC_E$ and $DUA_E$ (μmol C $L^{-1}$) were obtained by multiplying the concentrations values (μmol $L^{-1}$) by the number

of carbon per mole of compounds used as standards during calibrations (i.e phthalate and galacturonic acid, respectively).

## Oxidation Experiments

The Fe(II) oxidation experiments were performed in a double-jacketed thermostatic vessel (250 mL) at constant temperature of 25 ± 0.02°C using an AG-2$^{TM}$ bath. The pH was adjusted to the desired value to keep the pH constant to ± 0.01 during the experiment, through small additions of HCl (0.1 M; analytical grade previously quartz distilled, Q-HCl) using an automatic titration system (Titrino 719S, Metrohm). The pH (free hydrogen ion scale, $pH_F$ =-log[$H^+$]) was determined at 25°C with an Orion pHmeter (Thermo Scientific), calibrating the combination glass electrode with tris(hydroximethyl)-aminomethane (Tris)–artificial seawater buffers (Millero, 1986). The samples were analyzed in triplicate and the average results were calculated. The addition of a fixed concentration (25 nM) of Fe(II) to the sample corresponded to the zero time of the reaction. The kinetic experiments were carried out under dark conditions in order to avoid both the photo-reduction of organically complexed Fe(III) (Kuma et al., 1995) and the photo-generation of $H_2O_2$ (Steigenberger et al., 2010) from natural exudates which can produce redox interactions with iron. The samples were mixed at 120 rpm with a Teflon-coated magnetic stirrer.

In order to investigate the effect of DUA on Fe(II) oxidation, avoiding the presence of other organic ligands that could interfere in the interaction of Fe(II) with DUA, glucuronic acid was selected as ligand model. Glucuronic acid (Sigma-Aldrich) was added to 200 mL of ASW (S = 35). The concentrations of glucuronic acid (0–1,000 nM) and pH (pH 7.75 and 8.25) were independently varied during the oxidation studies, assuming the studies performed in ASW without ligand addition as the reference value (control). The solutions were brought to experimental temperature (25°C) under air saturated conditions by bubbling the solution with pure synthetic air for 1 h prior to starting the oxidation studies. The dissolved [$O_2$] was determined from solubility equations (Benson and Krause, 1984). However, to study the behavior of Fe(II) in the presence of ligands released by *E. huxleyi* under different $CO_2$ scenarios, SWEN and SWEX were not bubbled with pure air in order to avoid alterations of carbonate chemistry generated in the microcosms and because of that, the oxygen concentrations were measured before the kinetic studies.

## Fe(II) Analysis

Iron concentrations in the samples were determined by UV–VIS spectroscopy using a colorimetric method (Viollier et al., 2000) and modified by Santana-Casiano et al. (2005) in order to measure Fe(II) at nanomolar concentrations. The stock Fe(II) solution ($4 \times 10^{-4}$M) was prepared in a saline matrix (NaCl, 0.7 M), using ammonium iron(II) sulfate hexahydrate (Sigma). The working Fe(II) solutions were prepared in 2 mM Q-HCl to prevent Fe(II) oxidation while remaining low enough to avoid significant pH change that might alter the kinetic experiments when iron was added. The solutions of disodium salt of 3-(2-pyridyl)-5,6-bis(4-phenylsulfonic acid)-1,2,4-triazine (Ferrozine, 0.01 M) and sodium fluoride (0.001 M) were prepared weekly and kept in the fridge until their use in the kinetic experiments. The measurements of Fe(II) were carried out following the ferrozine method because it allows us to monitor the full-spectra over time and if any intermediate or interaction is produced, it can be taken into account during the assay. Ferrozine reacts rapidly with Fe(II), forming a water soluble complex, which forms a stable peak at 652 nm in the pH range 4–9. Moreover, this technique is not affected by the presence of high levels of dissolved organic matter (Pullin and Cabaniss, 2003; González et al., 2014). The use of Ferrozine as an iron complexing agent can promote deviations in the Fe(II) measurements (Hopwood et al., 2017a), due to the formation and reduction of an Fe(III)-Ferrozine complex (Hudson et al., 1992). However, in the presence of NaF, Ferrozine does not bind Fe(III) to a significant degree (Santana-Casiano et al., 2005; González et al., 2016) and, therefore a stable absorbance can be read for over 20 min.

At each selected time, 10 mL of sample were withdrawn from reaction vessels to a 25 mL glass flask containing the reagents (Santana-Casiano et al., 2005). The absorbance was read with a 5 m long waveguide capillary flow cell (World Precision Instruments$^{TM}$) connected to the UV–VIS detector USB2000 (Ocean Optics$^{TM}$). The detection limit of the instrument was 0.8 nM of Fe(II) calculated as three times the standard deviation of the lowest calibration value ($n = 3$; 5 nM Fe(II)). The light used was a halogen light source (HL-2000-FHSAfrom Mikropack). The capillary flow cell and the detector were connected using an optical fiber. The spectra were recorded using the OOIBase32 software by Ocean Optics. The samples were introduced into the column using a peristaltic pump (EXPETEC Perimax 12) with a flux of 1 mL/min. All dilutions were prepared with Milli-Q water (18 MΩ) and the chemicals used for the Fe(II) determination were trace analytical grade.

## Oxygen Measurements

The dissolved oxygen content in the experimental cultures was determined during the 2nd, 5th and 8th day, by the modified Winkler's method (DOE, 1994) and expressed as μmol $L^{-1}$. The potentiometric detection of the end point of titration was carried out using a programmed Metrohm Titrino.

## Oxidation Kinetic Theory

At micromolar and nanomolar levels, the most broadly accepted mechanism (Equations 1–4) for the oxidation of inorganic Fe(II) by $O_2$ is the Haber–Weiss sequence.

$$Fe\,(II) + O_2 \rightarrow Fe\,(III) + O_2^{\cdot -} \quad (1)$$

$$Fe\,(II) + O_2^{\cdot -} + 2H^+ \rightarrow Fe\,(III) + H_2O_2 \quad (2)$$

$$Fe\,(II) + H_2O_2 \rightarrow Fe\,(III) + OH^{\cdot} + OH^- \quad (3)$$

$$Fe\,(II) + OH^{\cdot} \rightarrow Fe\,(III) + OH^- \quad (4)$$

The presence of organic ligands (L) means reaction 5 may take place and the generation of reactive oxygen species (Equations 1–4) may be strongly affected (Miller et al., 2012), since the organic complexed ferrous iron can be oxidized to form the corresponding ferric complex (Equation 6) modifying the

generation of those redox reactive species.

$$Fe\,(II) + L \leftrightarrow Fe\,(II)\,L \quad (5)$$

$$Fe\,(II)\,L + O_2 \rightarrow Fe\,(III)\,L \quad (6)$$

Nevertheless, the Fe(II) oxidation rate equation in the presence of oxygen is defined by equation 7, as an apparent oxidation rate ($k_{app}$, $M^{-1}$ $min^{-1}$), independent of the mechanism describing the process (Santana-Casiano et al., 2005).

$$\frac{d\,[Fe\,(II)]}{dt} = -k_{app}\,[Fe\,(II)]\,[O_2] \quad (7)$$

Under air saturated conditions, the slope of the logarithmic Fe(II) concentration as a function of reaction time, using a least-squares linear regression, gave the pseudo-first order rate, which is defined according to equation 8.

$$\frac{d\,[Fe\,(II)]}{dt} = -k'\,[Fe\,(II)] \quad (8)$$

where $k' = k_{app}\,[O_2]$.

## Data Treatment and Numerical Model

R Development Core Team (2013) was used for statistical computing. Statistical differences in $[O_2]$, $DOC_E$ and Fe(II) oxidation rates were evaluated using two-way analysis of variance (ANOVA), in order to avoid a significant result occurring due to random chance. The assumptions of normality and homoscedasticity were verified using the Shapiro-Wilk and Barlett tests respectively. Regression models were used to assess the relationship between the Fe(II) oxidation rate, $DOC_E$, $DUA_E$, and pH. For all statistical analyses, a probability level of $\alpha = 0.05$ was considered.

A kinetic model was developed using the Gepasi software (Version 3.30). A response surface methodology (Santana-Casiano et al., 2005) was considered, together with initial $pH/pCO_2$ conditions and all redox, dissociation and equilibrium constants for the reaction of Fe(II) species with the major inorganic species in seawater (Samperio-Ramos et al., 2016). The kinetic model was broadened to include the interaction between nutrients and Fe(II) (Samperio-Ramos et al., 2016). The $k_i$ values of Fe(II) organic complexes were obtained by adjusting experimental Fe(II) concentrations/time pairs of data to the model output as indicated elsewhere (Santana-Casiano et al., 2005).

# RESULTS

The kinetic studies were performed in seawater enriched with nutrients (SWEN) and seawater enriched with nutrients and exudates of *E. huxleyi* (SWEX), in order to determine the effect of organic ligands released under different pH conditions.

## DOC Dependence

To demonstrate that the total organic ligands exuded during the microalgae growth can be indirectly related to organic matter released (Strmečki et al., 2010; González et al., 2014), the dissolved organic carbon exuded ($DOC_E$) by *E. huxleyi* has to be monitored under different $pH/pCO_2$ conditions. Thus, $DOC_E$ was determined on the 2nd, 5th and 8th days of growth, representing the three growth stages (i.e., LP, EP, and SP respectively). During the LP, no significant production of DOC was detected (two-way ANOVA: $p = 0.9448$), demonstrating that the organic exudation correlated with the *E. huxleyi* growth (Biddanda and Benner, 1997). Additionally, the net production of DOC did not show significant differences among the pH conditions in the different growth stages (two-way ANOVA: $p = 0.9703$), in accordance with previous results (Borchard and Engel, 2012, 2015).

At pH 8.10 the oxidation rate of Fe(II) (25 nM) in the ESTOC surface seawater enriched with nutrients (SWEN) was $3.18 \pm 0.02$ $M^{-1}$ $min^{-1}$ and the Fe(II) half-life reached 2.4 min. During the LP the $k_{app}$ (**Table 1**) did not change significantly (two way ANOVA: p=0.7070) with respect to SWEN (control). The increase of DOC in the SWEX, from exponential phase, was followed by a corresponding decline in the oxidation rate, reaching minimum values at maximum $DOC_E$ (**Table 1** and **Figure 1**). These results indicated that the presence of organic compounds excreted by the coccolithophorids under different $pH/pCO_2$ conditions affected the rate of oxidation of Fe(II) (**Figure 1**). The experimental data of log $k_{app}$ were fitted to an exponential decay as a function of $DOC_E$, for each acidification scenario (**Table 2**).

**Figure 2** shows that the variability on Fe(II) oxidation rate, due to the presence of exudates ($\Delta \log k_{app}^{DOC_E} = \log k_{app}^{SWEN} - \log k_{app}^{SWEX}$), was not constant over the entire pH range studied. During SP, the $\Delta \log k_{app}^{DOC_E}$ increased as the pH diminished, from $0.14 \pm 0.01$ $M^{-1}$ $min^{-1}$ (pH = 8.25) to $0.22 \pm 0.02$ $M^{-1}$ $min^{-1}$ (pH = 7.75) (**Figure 2**). This was equivalent to a decrease of between 27% (pH = 8.25) and 40% (pH = 7.75) in $k_{app}$. Thus, the presence of exudates increased the half-life time ($t_{1/2}$) up to 0.7 min, 1 min, 2 min and 2.7 min for pH 8.25, 8.10, 7.90, and 7.75 respectively (**Table 1**). The experimental results of Fe(II) oxidation rates ($M^{-1}$ $min^{-1}$) were fitted to a second order equation as a function of pH and $[DOC_E]$ (Equation 9), where $r^2$ was 0.987 and the standard error of the estimation in log $k_{app}$ was 0.03.

$$\log k_{app} = 24.87\ (\pm 1.68) - 6.48\ (\pm 0.42)\ pH + 0.48\ (\pm 0.03)\,pH^2 - 1.2 \cdot 10^{-3}\ \left(\pm 10^{-4}\right)\ [DOC_E] \quad (9)$$

While the maximum difference in the oxidation rates, due to changes in pH conditions ($\Delta log k_{app}^{pH} = \log k_{app}^{pH=8.25} - \log k_{app}^{pH=7.75}$) was $0.50 \pm 0.02$ $M^{-1}$ $min^{-1}$ in SWEN, the $\Delta log k_{app}^{pH}$ increased up to $0.59 \pm 0.04$ $M^{-1}$ $min^{-1}$ in the SP ($141.11 \pm 10.27$ μmol C $L^{-1}$), reducing the $k_{app}$ by 68% and 75%, respectively. The $t_{1/2}$ (**Table 1**) of Fe(II) increased in response to $CO_2$ enrichment both in SWEN (3.4 min) and SWEX (4.2 min and 6.0 min for $33.18 \pm 3.78$ μmol C $L^{-1}$ and $141.11 \pm 10.27$ μmol C $L^{-1}$, respectively). The effect of pH on the Fe(II)

**TABLE 1 |** Pseudo-first order oxidation rate ($k'$), apparent oxidation rate (log $k_{app}$) and half-life time ($t_{1/2}$) of Fe(II) under different pH conditions for seawater enriched with nutrients (SWEN) and seawater enriched organic exudates (SWEX).

| Media | pH | $[DOC_E] \pm SE$ ($\mu mol\ C\ L^{-1}$) | $[DUA_E]^b \pm SE$ ($nmol\ L^{-1}$) | $k' \pm SE$ ($min^{-1}$) | $[O_2]^c \pm SE$ ($\mu mol\ L^{-1}$) | log $k_{app} \pm SE$ ($M^{-1}\ min^{-1}$) | $t_{1/2}$ (min) |
|---|---|---|---|---|---|---|---|
| SWEN (Control) | 8.25 | – | – | 0.45 ± 0.03 | 196.27 ± 3.01 | 3.36 ± 0.03 | 1.5 |
| | 8.10 | – | – | 0.29 ± 0.01 | 194.30 ± 1.29 | 3.18 ± 0.02 | 2.4 |
| | 7.90 | – | – | 0.19 ± 0.02 | 194.78 ± 0.84 | 2.99 ± 0.03 | 3.7 |
| | 7.75 | – | – | 0.14 ± 0.01 | 191.26 ± 1.11 | 2.86 ± 0.02 | 4.9 |
| SWEX from LP | 8.25 | a | a | 0.44 ± 0.03 | 198.38 ± 2.86 | 3.35 ± 0.03 | 1.6 |
| | 8.10 | a | a | 0.30 ± 0.02 | 193.25 ± 3.70 | 3.19 ± 0.02 | 2.3 |
| | 7.90 | a | a | 0.18 ± 0.01 | 190.90 ± 3.69 | 2.97 ± 0.04 | 3.9 |
| | 7.75 | a | a | 0.15 ± 0.01 | 191.40 ± 2.30 | 2.88 ± 0.03 | 4.7 |
| SWEX from EP | 8.25 | 30.95 ± 4.52 | 73.09 ± 11.13 | 0.38 ± 0.02 | 194.78 ± 0.77 | 3.29 ± 0.02 | 1.8 |
| | 8.10 | 36.82 ± 11.85 | 83.43 ± 12.84 | 0.24 ± 0.01 | 201.13 ± 0.80 | 3.08 ± 0.03 | 2.9 |
| | 7.90 | 35.91 ± 8.66 | 89.70 ± 24.69 | 0.15 ± 0.02 | 199.00 ± 3.52 | 2.91 ± 0.03 | 4.5 |
| | 7.75 | 29.04 ± 9.94 | 66.45 ± 13.97 | 0.11 ± 0.02 | 195.14 ± 1.35 | 2.77 ± 0.05 | 6.0 |
| SWEX from SP | 8.25 | 130.89 ± 21.07 | 329.69 ± 29.02 | 0.33 ± 0.02 | 191.26 ± 1.11 | 3.23 ± 0.03 | 2.1 |
| | 8.10 | 147.77 ± 17.07 | 417.63 ± 13.84 | 0.20 ± 0.01 | 193.44 ± 3.28 | 3.00 ± 0.04 | 3.6 |
| | 7.90 | 151.87 ± 8.18 | 439.76 ± 20.27 | 0.13 ± 0.01 | 191.84 ± 3.76 | 2.81 ± 0.02 | 5.5 |
| | 7.75 | 133.93 ± 11.39 | 406.04 ± 42.58 | 0.09 ± 0.01 | 189.84 ± 4.07 | 2.64 ± 0.03 | 8.1 |

*The dissolved oxygen, as well as the dissolved uronic acids and dissolved organic carbon exuded by Emiliania huxleyi ($[DUA_E]$ and $[DOC_E]$, respectively) were monitored during the different growth stages (LP, lag phase; EP, exponential phase and SP, stationary phase). The temperature (25°C) and salinity (36.48) were kept constant (25°C). ± SE represents the standard error of the estimate in triplicate samples for all experiments.*

[a] *No significant differences with control seawater.*

[b] *DUA considered as hexoses (i.e., hexuronic acids).*

[c] *No significant differences.*

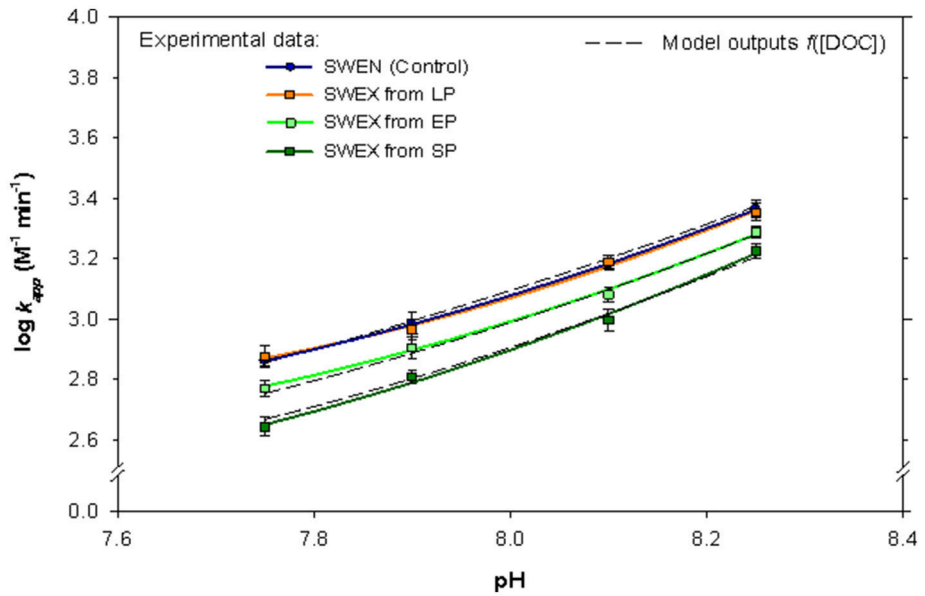


**FIGURE 1 |** Fe(II) oxidation rate constant as a function of pH for the seawater and the seawater enriched with the organic exudates (SWEX) excreted by *E. huxleyi* during the different growth stages (LP, lag phase; EP, exponential phase and SP, stationary phase). Temperature (25°C) and salinity (36.48) were kept constant. Error bar denoted standard error of the estimate (SE = ± SD/√n), $n = 3$).

**TABLE 2 |** Relationship between Fe(II) oxidation rate (log $k_{app}$) and dissolved organic carbon exuded ([$DOC_E$]) by *E. huxleyi*.

| pH | log $k_{app}$ ($M^{-1}$ $min^{-1}$) | $r^2$ | ± SE |
|---|---|---|---|
| 8.25 | $3.20\ (\pm0.02) + 0.16\ (\pm0.02)^{0.02\left(\pm10^{-3}\right)[DOC_E]}$ | 0.936 | 0.03 |
| 8.10 | $2.98\ (\pm0.01) + 0.20\ (\pm0.01)^{0.02\left(\pm10^{-3}\right)[DOC_E]}$ | 0.978 | 0.01 |
| 7.90 | $2.78\ (\pm0.03) + 0.21\ (\pm0.03)^{0.01\left(\pm10^{-3}\right)[DOC_E]}$ | 0.960 | 0.02 |
| 7.75 | $2.61\ (\pm0.04) + 0.25\ (\pm0.03)^{0.01\left(\pm10^{-3}\right)[DOC_E]}$ | 0.959 | 0.02 |

*Organic material was excreted in seawater under different pH conditions. ±SE denotes standard error of the estimate.*

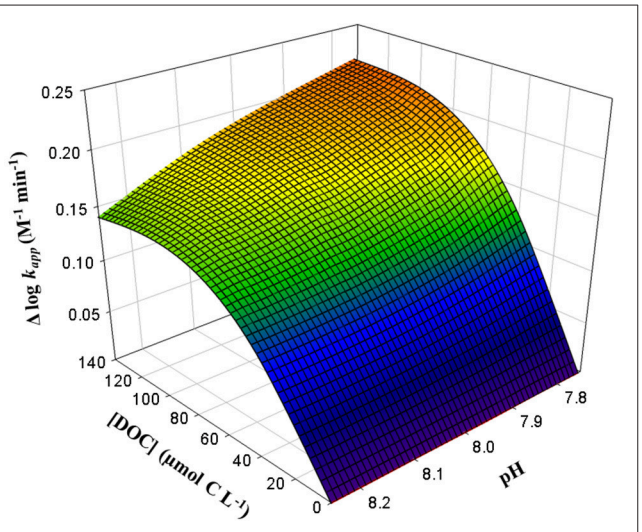


**FIGURE 2 |** Maximum increase for Fe(II) oxidation rate ($\Delta\log k_{app} = \log k_{app}^{SWEN} - \log k_{app}^{SWEX}$) by the presence of organic ligands (considered in the $DOC_E$) produced by *E. huxleyi* under different pH treatments. Temperature (25 °C) and salinity (36.48) were kept constants.

oxidation rate only as a result of the exudates was calculated (Eq 10) by subtracting the log $k_{app}$ values in SWEN and those in equation 13 for the growth phases, where the DOC was accumulated in the present study. $R^2$ was 0.952, and the standard error of the estimate was 0.03.

$$\Delta log\ k_{app} = 3.9 \cdot 10^{-2}\ \left(\pm 3.4 \cdot 10^{-3}\right)\ pH - \ 5 \cdot 10^{-3}\ \left(\pm 4 \cdot 10^{-3}\right) pH^2 + 10^{-3}\ \left(\pm 10^{-4}\right)\ [DOC_E] \quad (10)$$

Equation 10 permits determining the changes in the oxidation process in a context of ocean acidification and in the presence of ligands excreted by the *E. huxleyi*. In order to explain what ligands condition the oxidation process, it is advised to perform detailed studies of Fe(II) oxidation with individual model ligands. $DUA_E$ account for an important fraction of the $DOC_E$, ranging between 1 and 5% of the DOC released by *E. huxleyi* under different simulated pH conditions (Borchard and Engel, 2015; Samperio-Ramos et al., 2017). Thus, to elucidate the role played by $DUA_E$ in the SWEX, the next series of experiments were carried out using a simplified ligand model (i.e., glucuronic acid as DUA) in artificial seawater (ASW).

## Oxidation Rate in Presence of Uronic Acids

Oxidation rates, as well as the half-life time of Fe(II) are presented in **Table 3**. Fe(II) oxidation rates vary depending on L:Fe ratios and pH in solution. The addition of glucuronic acid did not significantly increase the oxidation rates between both pH conditions (two-way ANOVA; $p = 0.4114$), suggesting that the complexation of Fe(II) by DUA is relatively low. Figure S1 shows that the pseudo-first oxidation rates ($min^{-1}$) vary linearly with increasing molar ratio of DUA:Fe(II), implying that the reaction is of first order with respect to the ligand concentration. However, the results indicated that uronic ferrous complexes behaved differently depending on the pH conditions to which they were exposed, since the oxidation process is more sensitive to changes in the concentration of DUA at pH 7.75 than at pH 8.25. The experimental data ($k'$, $min^{-1}$) were fitted as a function of glucuronic acid concentrations and pH (Equation 11).

$$k' = -5.37\ (\pm0.05) + 0.70\ (\pm0.01)\, pH + 0.35 \cdot 10^{-4}\ \left(\pm0.01 \cdot 10^{-4}\right)[DUA] \quad (11)$$

The $r^2$ and the standard error of estimate were 0.999 and ±0.01, respectively. This equation can be used and applied under the experimental conditions fitted (i.e., pH = 7.75–8.25 and [DUA] = 0–1,000 nM).

## Modeling Approach for Oxidation Rates of DUA in a Context of Marcus Theory

We used the experimental results from section Oxidation rate in presence of uronic acids and the modeling approach described by Santana-Casiano et al. (2005), including the interaction between the glucuronate species ($CHO^-$) and the major divalent cations present in ASW, (i.e., $Ca^{2+}$ and $Mg^{2+}$) (Table S1). The model explains the reaction between Fe(II) and uronic acids (CHO) in terms of the fully deprotonated ligand state. In order to describe the experimental pH range considered (7.75–8.25), it is necessary to include the protonation equilibria of glucuronic acid. Potentiometric measurements support the conclusion that binding between uronic acids and divalent cations involves the carboxylate moiety as the main coordination center (Papageorgiou et al., 2010). Thus, the acidity constant of glucuronic acid (Table S1) was obtained from Jastrzab

**TABLE 3 |** Pseudo-first order rate ($k'$ $min^{-1}$) and half-life time ($t_{1/2}$) for Fe(II) (25 nM) oxidation at pH 8.25 and 7.75 in artificial seawater (ASW, $S = 35$) only and in presence of model dissolved uronic acid ligand (DUA: glucuronic acid) in concentrations from 25 to 1,000 nM (ligand to Fe ratio, L:Fe 1–40).

| [DUA] (nM) | L:Fe ratio | pH 8.25 | | | pH 7.75 | | |
|---|---|---|---|---|---|---|---|
| | | Oxidation rate $k'$ ($min^{-1}$) | ± SE | $t_{1/2}$ (min) | Oxidation rate $k'$ ($min^{-1}$) | ±SE | $t_{1/2}$ (min) |
| 0 (Control) | 0 | 0.428 | 0.004 | 1.62 | 0.068 | 0.002 | 10.12 |
| 25 | 1 | 0.430 | 0.009 | 1.61 | 0.071 | 0.004 | 9.71 |
| 100 | 4 | 0.432 | 0.009 | 1.60 | 0.076 | 0.003 | 9.13 |
| 250 | 10 | 0.435 | 0.008 | 1.59 | 0.083 | 0.007 | 8.35 |
| 500 | 20 | 0.443 | 0.006 | 1.57 | 0.094 | 0.006 | 7.35 |
| 1,000 | 40 | 0.450 | 0.011 | 1.54 | 0.117 | 0.008 | 5.92 |

*Temperature was kept constant (25°C). ±SE denotes the standard error of the estimate in triplicate samples for all experiments.*

et al. (2016). Taking into account the experimental conditions previously described, the equilibrium constant (Equation 12) for uronate ligand (denoted in the model as $CHO^-$) and Fe(II), as well as the corresponding oxidation reaction of the $FeCHO^+$ complex (Equation 13) were adjusted in order to produce the best agreement between the experimental data and the model outputs (Figure S1).

$$Fe^{2+} + CHO^- \leftrightarrow FeCHO^+ \quad (12)$$

$$Log\ K_{\mathrm{FeCHO+}} = 3.68 \pm 0.81 M^{-1}$$

$$FeCHO^+ + O_2 \rightarrow FeCHO^{2+} + O_2^- \quad (13)$$

$$Log\ k_{\mathrm{FeCHO+}} = 3.28 \pm 0.41 M^{-1} min^{-1}$$

The electron transfer in the oxidation of organic Fe(II) complexes by oxygen, is accomplished by an outer-sphere mechanism, through the precursor complex, without any variation in the inner sphere of the molecule. Marcus theory connects these outer-sphere electron-transfer mechanisms with the free energy of the oxidation reaction. Additionally, it is possible to delimit the free energy of reaction 13 following the equation (Equation 14) described by Tratnyek and Hoigné (1994).

$$k_i = \frac{k_d}{1 + \frac{k_d}{K_d Z}\, exp\left[\frac{\frac{\lambda}{4}\left(1+\frac{\Delta G^\circ}{\lambda}\right)^2}{RT}\right]} \quad (14)$$

*where* $k_d$ is the diffusion-controlled limit ($10^{10}$ $M^{-1}$ $s^{-1}$), R is the universal gas constant and T is the temperature (°K). The term $k_d/K_dZ$ has a constant value of 0.1 (King and Farlow, 2000) and $\lambda$ is a fitting parameter related to the energy required to rearrange the transition state without electron transfer occurring, being 103 kJ $mol^{-1}$ for organometallic compounds (Rose and Waite, 2003). The individual oxidation rate of $FeCHO^+$ species provides a standard free energy, $\Delta G^0$ of 37.45 ± 1.58 kJ $mol^{-1}$. The reduction of oxygen to superoxide follows the Franck-Condon principle, which defines the oxidation process as an electronic transition without nuclear coordination modification. Therefore, from the $\Delta G^0$ calculated, it is possible to determine the half potential for reduction between Fe-CHO complexes ($E^0_{Fe-CHO}$).

$$\Delta G^\circ = -F(E^0_{o_2 \rightarrow o_2^-} - E^0_{FeCHO^{2+} \rightarrow FeCHO^+}) \quad (15)$$

where, F is the Faraday constant and $E^0_{o_2 \rightarrow o_2^-}$ in aqueous solutions oscillate between −0.16 and −0.20 V (Koppenol et al., 2010). Solving equation 12, the half potential for reduction of the Fe–CHO complexes ranged between 0.214 and 0.242 V. From the Nernst equation and using the corresponding value of $E^0_{FeL}$, the equilibrium constant ratio ($K_{FeCHO^{2+}}/\ K_{FeCHO^+}$) can be calculated.

$$E^0_{Fe-DUA} = E^0_{Fe} - 0.059 \log\left(\frac{FeCHO^{2+}}{FeCHO^+}\right) \quad (16)$$

Considering the standard half reaction potential for $E^0_{Fe} = 0.77\ V$, a $K_{Fe(III)-DUA}/K_{Fe(II)-DUA}$ ratio between $10^9$ and $10^{11}$ is obtained. Resolving the ratio $K_{FeCHO^{2+}}/\ K_{FeCHO^+}$ estimated from Marcus theory, the $logK_{FeCHO^{2+}}$ would limit between 13 and 16 $M^{-1}$.

## Kinetic Model Considering Exudates of *E. huxleyi* Produced Under Different pH Conditions

In line with previous studies (Samperio-Ramos et al., 2016), we have used a kinetic model to consider the Fe(II) oxidation process in seawater enriched with nutrients (SWEN) at 25°C (**Table 1**). The modeling approach also took into consideration the different $pH/pCO_2$ conditions fixed in the microcosms (Samperio-Ramos et al., 2017). In order to explain the key role played by the $FeCHO^+$ complex on speciation and overall oxidation rate of Fe(II) in SWEX, we assumed the equilibrium constants and the individual oxidation rate estimated with the DUA model ligand in section Oxidation rate in presence of uronic acids. Uronic acids derived from hexoses (i.e., glucuronic and galacturonic acids) are the main class of sugar acids present in the *E. huxleyi* exudates (Borchard and Engel, 2015) and, therefore the $DUA_E$, measured in the SWEX (Figure S2) were considered as hexuronic acids in the model (**Table 1**). Additionally, to describe the role played by the organic pool ligands in the Fe(II) redox behavior, a non-specific type ligand (denoted as L) was also included in the modeling approach.

The best fit between the model output and the experimental distribution, under the different $pH/pCO_2$ conditions set in the

microcosms, gave one ligand with two protonation constants described by the acid-base equilibria of Equations (17, 18).

$$LH_2 \leftrightarrow LH^- + H^+ \quad (17)$$
$$log\ K_a = 8.81 \pm 0.27 M^{-1} \quad (this\ work)$$

$$LH^- \leftrightarrow L^{2-} + H^+ \quad (18)$$
$$log\ K_a = 9.02 \pm 0.56 M^{-1} \quad (this\ work)$$

Taking into account all the experimental conditions shown in section DOC dependence, the Fe(II) complexation for the ligand, $L^{2-}$ (Equation 19), and its corresponding oxidation process (Equation 20) were included in the model. Both constants were determined empirically by the best fit of the model to experimental data, and reflect the complexation and oxidation of Fe(II) with natural ligands with different binding capacities and reactivity than CHO.

$$Fe^{2+} + L^{2-} \leftrightarrow FeL \quad (19)$$
$$log\ K_{FeL} = 11.64 \pm 1.15 M^{-1} \quad (this\ work)$$

$$FeL + O_2 \rightarrow FeL^+ + O_2^- \quad (20)$$
$$log\ k_{FeL} = 1.84 \pm 0.22 (M^{-1} min^{-1}) \quad (this\ work)$$

The oxidation rate of the Fe-L complex (Equation 20) was also studied in the context of Marcus theory providing a standard free energy of 50.47 ± 1.68 kJ $mol^{-1}$ and a range of half potential for reduction between +0.304 and +0.378 V. Considering the equilibrium constant of reaction 19 and the $K_{Fe(III)-L}/K_{Fe(II)-L}$ ratio computed ($10^7$-$10^8$ $M^{-1}$) from Nernstian theory (Equation 16), a wide range of possible $K_{Fe(III)-L}$ ($10^{17}$-$10^{21}$ $M^{-1}$) are obtained.

The best fitting concentrations for L type-ligands during the EP were 16 ± 3 nM (pH = 8.25), 21 ± 2 nM (pH = 8.10), 22 ± 6 nM (pH = 7.90), and 18 ± 2 nM (pH = 7.75). During the SP, the concentrations of L included in the model were 49 ± 6, 56 ± 11, 62 ± 8, and 55 ± 8 nM for a pH of 8.25, 8.10, 7.90, and 7.75, respectively.

Because the photochemical production rate of $H_2O_2$ is directly related to the presence of organic matter (Steigenberger et al., 2010), a generation rate of 0.04 nM (μmol C)$^{-1}$ $day^{-1}$ (Price et al., 1998) during the experimental cultures was included in the model. The concentrations of $H_2O_2$ achieved were 24.1 ± 0.1 nM, 40.9 ± 0.4 nM, and 86.7 ± 1.9 nM for lag (2nd day), exponential (5th day) and stationary (8th day) growth phases, respectively.

The oxidation processes are formed of parallel reactions in which the individual species interact at different rates with each oxidizing agent (González et al., 2016). The Fe(II) oxidation rate (Equation 21) can be determined as a function of the weighted sum of the oxidation rates of the individual ferrous species.

$$\begin{aligned} k_{app} = {} & k_{Fe^{2+}}\alpha_{Fe^{2+}} + k_{FeOH^+}\alpha_{FeOH^+} + k_{Fe(OH)2}\alpha_{Fe(OH)2} \\ & + k_{FeHCO3^+}\alpha_{FeHCO3^+} + k_{FeCO3}\alpha_{FeCO3} \\ & + k_{Fe(CO3)2}\alpha_{Fe(CO3)2} + k_{Fe(CO3)OH^-}\alpha_{Fe(CO3)OH^-} \\ & + k_{FeCl^+}\alpha_{FeCl^+} + k_{FeSO4}\alpha_{FeSO4} + k_{FePO4^-}\alpha_{FePO4^-} \\ & + k_{FeHPO4}\alpha_{FeHPO4} + k_{FeH2PO4^+}\alpha_{FeH2PO4^+} \\ & + \boldsymbol{k}_{FeCHO+}\alpha_{FeCHO+} + \boldsymbol{k}_{FeL}\alpha_{FeL} \end{aligned} \quad (21)$$

*where* $\alpha_i = [FeX_i] / [Fe(II)]_T$ denotes the molar fraction of each Fe(II) species in the solution, and *ki* are the individual rate constants for the Fe(II) species. Therefore, the kinetic model employed in the present study allow to calculate the Fe(II) speciation and the contribution of the individual species to the overall rate. Because no significant differences were found in DOC between SWEN (control) and SWEX during the LP (**Table 1**), the speciation and fractional contribution of the LP can be considered as not significantly different to of SWEN.

In SWEN and during the LP, the speciation under the different pH/$pCO_2$ conditions was controlled by $Fe^{2+}$ (**Figure 3**), changing from 37% (pH = 8.25) to 47% (pH = 7.75). The second most important species at pH 8.25, $FeCO_3$ (33%), decreased its molar fraction under simulated acidification conditions, reaching 19% at pH 7.75. Fe(II) speciation was strongly affected when the levels of organic ligands were significantly different to those in control seawater (i.e., EP and SP). During the SP, speciation was controlled by $Fe^{2+}$ and FeL, which were the most important species between pH 8.25 and pH 8.15, reaching 33 and 28%, respectively (**Figure 3**). On the contrary, the role played by the $FeCHO^+$ complex in the speciation was secondary (0.1–0.5%) although it became more important as the ligand concentration and the pH decreased (data not shown).

**Figure 4** shows the contributions of the different Fe(II) species to the Fe(II) oxidation rate with $O_2$. The oxidation processes in SWEN and SWEX during the LP, were controlled by $FeH_3SiO_4^+$, from pH 7.75 (23%) to pH 7.85 (22%) and by the $Fe(OH)_2$ and from pH 7.86 (21%) to pH 8.25 μatm (42%). The presence of organic ligands changed the contribution of each individual species to the overall Fe(II) oxidation rate across the pH/$pCO_2$ conditions exposed during the cultures (**Figure 4**). $Fe(OH)_2$ continues to be the most important contributor from pH 7.83 (17%) to pH 8.25 (37%) during the EP and from pH 8.08 (24%) to pH 8.25 (33%) during the SP, while the contribution of $FeCHO^+$ rose from 5% (pH 8.25) to 16% (pH 7.75) during the EP and became to be the most important species between pH 7.75 (35%) and 7.95 (22%) during the SP. Additionally, during the EP the maximum contribution for the FeL complex reached 10% (pH 8.25) and it was the most important contributing species from pH 7.96 (22%) to pH 8.07 (23%) during the SP.

# DISCUSSION

## Kinetic Studies

The oxidation kinetics of Fe(II) in seawater are significantly faster in presence of high concentrations of silicate due to the role played by the Fe(II)-silicate complexes on the overall oxidation

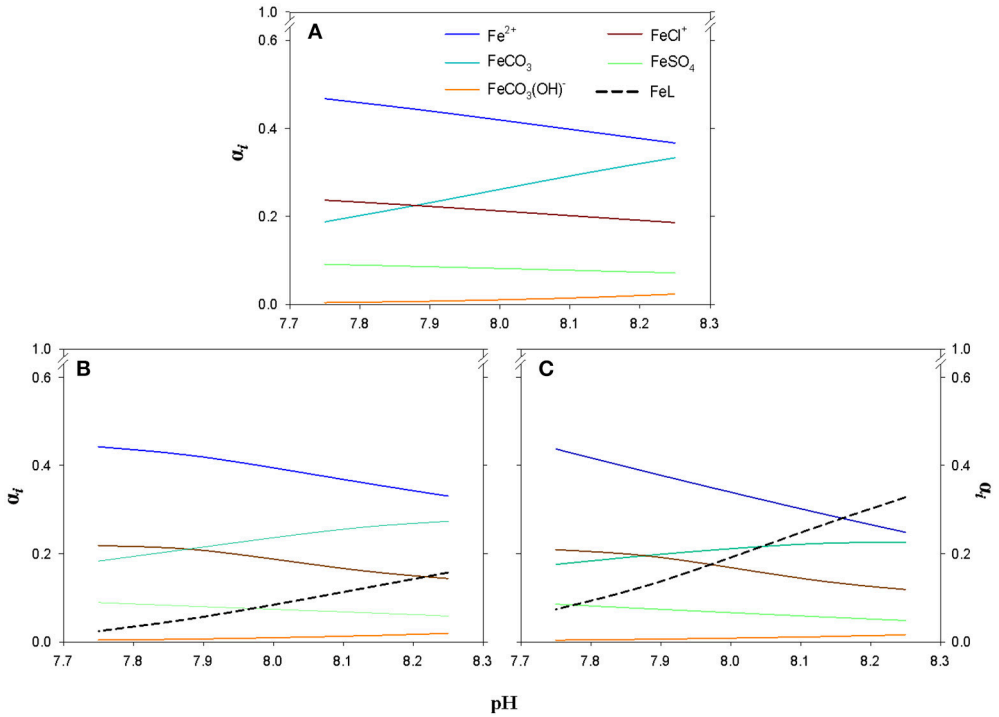


**FIGURE 3 |** Fe(II) speciation from the kinetic modeling approach: **(A)** seawater enriched with organic ligands present and excreted during the lag phase (LP = 0–2 days), **(B)** exponential phase (EP = 3–5 days with $[DOC_E] = 33.18 \pm 3.78$ μmol C · $L^{-1}$), and **(C)** stationary phase (SP = 6–8 days with $[DOC_E] = 141.11 \pm 10.27$ μmol C · $L^{-1}$) in cultures of *E.huxleyi* under different pH conditions ($T^a = 25°C$ and S = 36.48).

process (Samperio-Ramos et al., 2016). The results obtained in SWEN are close to those from other studies carried out with North Atlantic seawater enriched with nutrients (González et al., 2014; Samperio-Ramos et al., 2016), confirming that the silicate affected the Fe(II) oxidation rate and the lifetime of Fe(II). This study also shows a lessening in the oxidation rate of Fe(II) due to the presence of the organic ligands released from the coccolitophorid *E. huxleyi*, proving that the organic matter exuded by phytoplankton can preserve Fe(II) for longer periods in oxygen rich waters, as a result of the formation of ferrous organic complexes (Rijkenberg et al., 2006; Roy et al., 2008; Breitbarth et al., 2009a; González et al., 2014).

As has previously been demonstrated (Santana-Casiano et al., 2000; Pullin and Cabaniss, 2003; González et al., 2016), the oxidation rate decreases as a function of the pH (**Figure 2**), giving minimum oxidation rates at the higher values of studied pH. The data presented here are also comparable with those obtained by Breitbarth et al. (2009a) during a coastal seawater mesocosm experiment, where the authors linked the significant increase of Fe(II) half-life time to Fe(II) complexation by biologically mediated organic ligands, especially in the lower pH treatments. According to the results presented here (**Figure 1**), the organic iron ligands present in SWEX affect the kinetic behavior of iron in the pH-range studied, due to variations in the Fe(II) speciation. Therefore the decrease in the Fe(II) oxidation rate is directly linked to the production of organic compounds during the growth of *E. huxleyi* in each pH/$pCO_2$ treatment.

Ligands with carboxylic moieties are known to accelerate the effective oxidation rate of the reaction by forming complexes with Fe(II) (Santana-Casiano et al., 2000; Pham and Waite, 2008). At pH 6.0, citrate causes an increase in the Fe(II) oxidation, but at pH 8.0, the Fe(II) oxidation decreased (Pham and Waite, 2008). Nevertheless, the oxidation rate of Fe(II) did not show a significant response to DUA additions. The uncomplexed inorganic Fe(II), the more labile species to form organic complexes, dominates the Fe(II) speciation at pH lower than 7.8 (Samperio-Ramos et al., 2016). The hydrolysis of metal, which prevents the coordination with the carboxylic moieties, increase under the pH conditions here studied (Millero et al., 2009). Recently, Norman et al. (2015) showed that Fe(II)-complexes formed in the presence of EPS from *E. huxleyi* undergo rapid oxidation in relation to control seawater. Their results showed that the oxidation kinetics in the presence both of uronic acids and polysaccharides (i.e glucuronic acid and dextran, respectively) correlated significantly with those obtained for EPS from *E. huxleyi*. Contrary to this type of behavior, Kuma et al. (1995) determined that the addition of glucuronic acid to seawater from Funka Bay slightly slowed Fe(II) oxidation at micromolar levels. The specific interaction–ion-pairing model for Fe(II) speciation and oxidation by molecular oxygen is a function of pH, temperature and medium composition (Pullin and Cabaniss, 2003; González et al., 2016). In fact, the formation

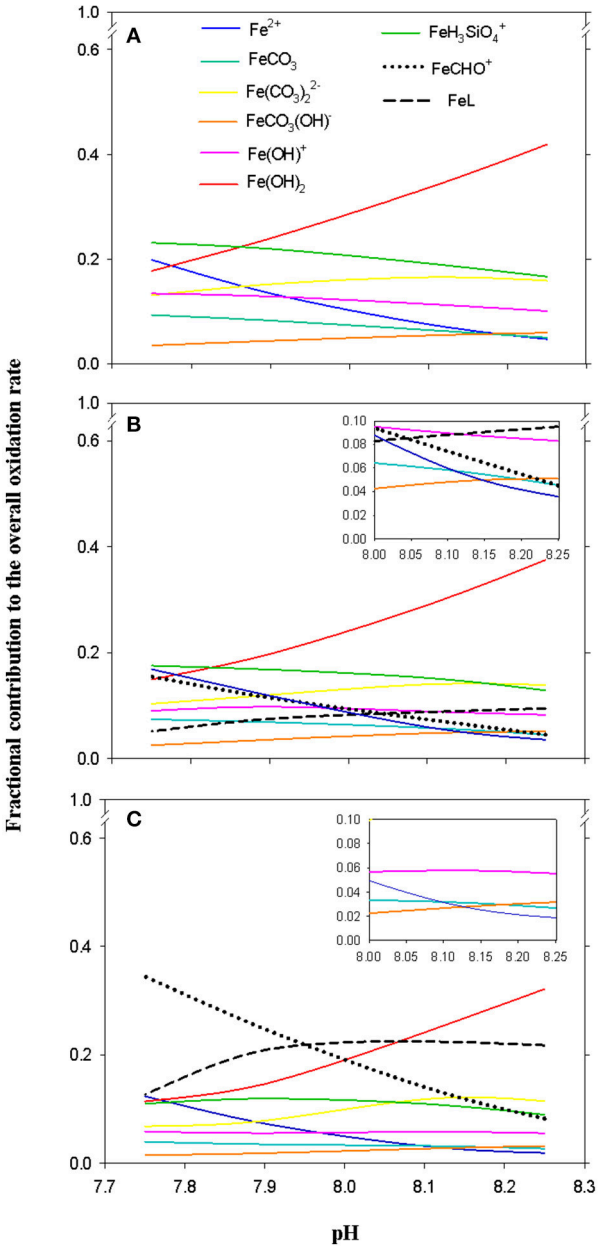


**FIGURE 4 |** Contribution of each Fe(II) species to the overall rate constant from the kinetic modeling approach: **(A)** seawater enriched with organic ligands present and excreted during the lag phase (LP = 0–2 days), **(B)** exponential phase (EP = 3–5 days with $[DOC_E] = 33.18 \pm 3.78$ μmol C · $L^{-1}$), and **(C)** stationary phase (SP = 6–8 days with $[DOC_E] = 141.11 \pm 10.27$ μmol C · $L^{-1}$) in cultures of *E.huxleyi* under different pH treatments ($T^a$ = 25°C and S = 36.48).

of Fe(II) complexes is dependent on the ligands binding capacities found in the medium. Therefore, the presence of other organic components in solution may modulate the influence of DUA in the redox behavior of Fe(II) due to competitive nature of complexing processes. It is often expected that a decrease by half a pH unit might result in a decrease in the percentage of ionized uronic ligands (Kohn and Kovác, 1978). In addition, a photo-induced hydrogen peroxide generation is found in the presence of saccharides (Steigenberger et al., 2010). In natural waters, $H_2O_2$ acts as a strong Fe(II) oxidant (Equation 3), influencing the Fe(II) redox chemistry (King and Farlow, 2000; González-Dávila et al., 2006; Miller et al., 2012; González et al., 2016). Therefore, it is difficult to make direct comparisons of our results with other studies carried out in natural seawater (Kuma et al., 1995; Norman et al., 2015), due to both the fixing of different physicochemical parameters for the experiments, such as temperature, light and pH, as well as, the lack of details of natural iron-ligands present in solution. For example, in Sub-Arctic Pacific ocean waters, Roy and Wells (2011) showed an acceleration of Fe(II) oxidation. The authors proposed that the presence of strong Fe(III) prokaryotic binding ligands (i.e., siderophores), increased the Fe(II) oxidation process. However, due to the significant saccharide concentrations (up to 30 μmol C $L^{-1}$) reported in Fe-limited regions (Pakulski and Benner, 1994), as well as the high content of uronic acids detected in the colloidal matrix of the bacterioplanktonic EPS (Decho and Gutierrez, 2017), our results suggest that DUA might have contributed to the enhanced overall oxidation rate observed by Roy and Wells (2011). In this work, the presence of $DUA_E$ did not result in an increase of the oxidation rate, suggesting that *E. huxleyi* exudates include other types of organic ligands that are capable of binding Fe(II) and slowing the oxidation process. For example, phenolic compounds such as catechin and sinapic acid are part of the organic compounds exuded by eukaryote phytoplankton (Rico et al., 2013; López et al., 2015) that play an important role in the decrease of the Fe(II) oxidation rate (Santana-Casiano et al., 2014).

## The Kinetic Modeling Approaches

The specific kinetic model, used in this work for the interaction between Fe(II) and CHO, fits the data well over a wide range of concentrations of DUA under different ocean acidification conditions. To date, the only stability constant reported for Fe-saccharide in seawater ($10^{19}$ $M^{-1}$) has been for the iron-gluconate species (Croot and Johansson, 2000). Ferric binding uronic acids have been found to be undetectable with the competitive ligand exchange–adsorptive cathodic stripping voltammetry (Strmečki et al., 2010), the technique commonly used to delimit Fe complexation in seawater. Therefore, this analytical overlap suggests that CHO fall within the class of ligands with "weak affinity" for Fe ($<10^{20}$ $M^{-1}$) and defined as $L_4$ by Bundy et al. (2014). In turn, Baldi et al. (2009), by means of cyclic voltammetric and potentiostatic experiments, have estimated that the stability constant for Fe(III) and bacterial EPS might be in the range of 12–13 $M^{-1}$. Several studies have suggested that metal complexing capacities by EPS are due to the presence of DUA as binding sites (Baldi et al., 2009; Ozturk et al., 2014). The range of stability constants of the $FeCHO^{2+}$ complex, computed from equation 16, is slightly higher than that considered by Baldi et al. (2009). Nevertheless, the ability to chelate iron in EPS is related not only to the amount of anionic groups but also to the three-dimensional distribution of binding sites and their accessibility (Strmečki et al., 2010). These polymers

are characterized by a significant level of hydrophobicity, which is due to the presence of uncharged groups, such as ester-linked acetyl fractions, peptidic moieties and deoxysugars, which might decrease the effective binding capacity of uronic fractions. In addition, the value of the equilibrium constant for the $FeCHO^{+}$ complex fixed in the model is close to that obtained, through the potentiometric titration, for glucuronic acid and other divalent cations such as $Mg^{2+}$ or $Cu^{2+}$ (Jastrzab et al., 2016). Consequently, these results can be assumed to determine the role played by uronic acids in the speciation and overall oxidation rate of Fe(II) in presence of the *E. huxleyi* exudates produced under different pH/$pCO_2$ conditions.

However, the exudates of *E. huxleyi* discussed in the present work result from a mixture of saccharides, and other uncharacterized organic compounds that may react in different ways with iron. In fact, the study conducted by Boye and van den Berg (2000) with *E. huxleyi* cultures, under different Fe-bioavailability conditions indicated that the complexation of Fe(III) was dominated by a single ligand with stability constant higher than those estimated for $FeCHO^{2+}$ complex. Due to the high heterogeneity of *E. huxleyi* exudates, the oxidation rate, as well as the equilibrium and acidity constants, might represent an average value of the sum of the individual rates/constants weighted by the fraction of each species in solution (Rose and Waite, 2003). The theoretical range ($10^{17}$-$10^{21}$ $M^{-1}$) of the stability constant for the Fe(III)-L complex is in reasonable agreement with those found in the literature for ligands with bindings capacities lower than $L_1$ (Gledhill and Buck, 2012; Bundy et al., 2014; Gerringa et al., 2016), including those estimated by Boye and van den Berg (2000) in *E. huxleyi* cultures.

The acidity constants (Equations 17, 18) are in close alignment with those of -OH groups of phenolic compounds, (Herrero-Martínez et al., 2005) and –SH fractions of glutathione-containing ligands (Poole, 2015). Significant amounts of low molecular weight organic material with thiolic and phenolic fractions are known to be generated in cultures of microalgae (Vasconcelos et al., 2002; Rico et al., 2013; López et al., 2015), including *E. huxleyi* (Dupont and Ahner, 2005; Strmečki et al., 2010; Jin et al., 2015), although these ligands can be also present in solution as monomers due to photochemical breakdown (Laglera and van den Berg, 2006; Li et al., 2015; Lu et al., 2016). Moreover, both thiol- and hydroxy- groups have been described as one of the most active groups binding divalent cationic metals in aqueous solution (Hider and Kong, 2011).

The concentrations of non-specific ligands are within the range (5–114 nM) described by other authors in *E. huxleyi* cultures (Boye and van den Berg, 2000; Vasconcelos et al., 2002). In chemostat cultures of *E. huxleyi*, under acidification simulated conditions, Borchard and Engel (2012) determined similar levels of $DUA_E$ (180–400 nM) than those measured and fitted in this modeling approach during the SP (**Table 1**).

Due to the ability to promote competitive reactions, peroxide of hydrogen, superoxide and hydroperoxyl, may have a profound impact on the iron redox chemistry (González-Dávila et al., 2006; Wang and Liu, 2014). However, the role played by $H_2O_2$ and free radicals in the oxidation of organic complexes of Fe(II) is also relatively minor under oxygen saturated conditions (Miller et al., 2012). Other studies have showed that at nanomolar levels of Fe(II), $H_2O_2$ and $O_2$ compete in the oxidation of inorganic ferrous species (González-Dávila et al., 2006). In oligotrophic ocean waters, as the ESTOC site, the levels of $H_2O_2$ are generally less than 20 nM, below 200 m of depth (Hopwood et al., 2017b). With levels of $H_2O_2 < 125$ nM, oxygen saturated conditions and pH > 7.5, $O_2$ dominates the oxidation kinetics of inorganic species of Fe(II), since the $k_{app}$ by $O_2$ is proportional to $[OH^-]^2$ and the $k_{app}$ by $H_2O_2$ is proportional to $[OH^-]$ (Moffett and Zika, 1987; González-Dávila et al., 2006). Nevertheless, our model also included the role played by $H_2O_2$ and $O_2^-$ in the oxidation process, including the individual rates for Fe(II) for both species (Santana-Casiano et al., 2005; Samperio-Ramos et al., 2016).

The individual contribution of Fe(II)-silicate species (i.e., $FeH_3SiO_4^+$) to the Fe(II) overall oxidation rate, computed from the kinetic model, was important over the whole pH/$pCO_2$ range (**Figure 4**). However, the heterogeneous composition of the microbial exudates controls the formation of ion-pairs, as well as the reactivity of those organic components in solution, determining the oxidation kinetic rates of Fe(II). The model outputs for SWEX also showed that the influence of FeL diminished as pH decreased in the cultures. Recently, Gledhill et al. (2015) carried out a non-ideal competitive adsorption (NICA)–Donnan model, using phenolic and carboxylic moieties as binding components, to determine the chemical speciation of Fe and Cu in seawater as a function of pH. In line with our work, their results indicated a decrease in iron and copper binding by organic matter under higher-acidity conditions. Nevertheless, the individual contributions to the overall Fe(II) rate demonstrated that Fe(II).organic complexes played a key role in the Fe(II) oxidation process, especially when the natural ligands were produced under acidified conditions ($pCO_2$ > 400 μatm; pH < 8.07). On the other hand, the $DUA_E$ is affected by $CO_2$ supply and an increase in acidification conditions might stimulate the biosynthesis and release of sugar acids by coccolitophorids (Fukuda et al., 2014; Lee et al., 2016; Samperio-Ramos et al., 2017). Thus, the contribution of $DUA_E$, within the pool of organic ligands excreted by *E. huxleyi*, to the kinetic behavior of Fe(II) must be considered under a scenario of oceanic acidification, due to the role played by the $FeCHO^{+}$ complex on the oxidation rate at lower pH values.

## ENVIRONMENTAL IMPLICATIONS

The chemical behavior of iron in the ocean cannot be solely described by thermodynamics parameters, since the biological interactions and environmental forces prevent marine systems from reaching equilibrium. Measurements of iron redox kinetics in the presence of microorganism exudates, produced under controlled conditions, offer a new pathway to decipher the nature and reactivity of Fe complexing ligands in seawater, as well as the physico-chemical processes that regulate the microbial excretion.

This study suggests that DUA might favor the oxidation of Fe(II) to Fe(III) in the ocean. Although Fe(II) is the form of iron that is most easily assimilated by phytoplankton (Shaked and Lis, 2012), uronic ligands allow more disassociation and release

of labile iron, than strong iron ligands such as siderophores (Lis et al., 2015; Norman et al., 2015). Additionally, both unchelated Fe(III) and ferric-uronic complexes can be reduced to Fe(II) through physiological process (i.e., via surface ferric reductase activity) (Allen et al., 2008), photolytic reactions (Kuma et al., 1995) or interaction with reactive oxygen intermediates (Steigenberger et al., 2010; Wang and Liu, 2014). Therefore, the knowledge of the binding capacities and redox reactivity of iron and DUA are key parameters for a greater understanding of how $DUA_E$ enhances Fe(III) solubility and promotes Fe-uptake by microorganisms. This modeling approach for $FeCHO^+$ complexes can be used to discern the disparity between Fe(II) oxidation rates obtained in different oceanic regions (Roy et al., 2008; Breitbarth et al., 2009b; Roy and Wells, 2011; Norman et al., 2015; Santana-González et al., 2017) when the oxidation process is controlled by biologically occurring organic ligands. However, more laboratory studies with individual model ligands are needed in order to improve our knowledge about the role played by the different ligands, present in bacterio- and phytoplankton exudates, on the Fe(II) chemistry.

The Fe(II) oxidation process was a function of the complex composition of the organic ligands pool released by *E. huxleyi* under different pH conditions. The model output for iron-complexing ligands, with stability constant in close alignment to $L_2$, has been a common feature of these cultures either under low or high pH conditions. Thus, the extensive blooms of *E. huxleyi* (Engel et al., 2012), including those produced in high-$CO_2$ upwelling waters (Beaufort et al., 2011), might potentially be a source of $L_2$ to the ocean. Additionally, the presence of those ligands in the exudates excreted by *E. huxleyi* retard the oxidation process of Fe(II) in seawater, allowing Fe(II) to be present in solution for extended periods of time, as has been observed recently with other species of green alga (González et al., 2014) and cyanobacterium (Samperio-Ramos et al., 2018). Consequently, as responsible for decreasing the oxidation rate, phytoplanktonic exudates can play a decisive role in the biogeochemical cycle of iron in the surface layer of the ocean, making it more bioavailable.

Ocean acidification is a potential driver of change on marine organic matter dynamics because it influences primary production and microbial respiration (Piontek et al., 2013; Spilling et al., 2016). This study reveals new information on how the Fe-ligands, exuded under acidification conditions, might cause an important impact on the speciation, reactivity and bioavailability of iron in the future ocean. However, the findings derived from microcosms can introduce artifacts from experimental designs, such as the timescale conditioning of microorganisms to the manipulated environmental factors (Hurd et al., 2009). On the other hand, the acidification effect on $DOC_E$, and its chemical composition, might be small in relation to the background concentration and therefore, to be difficult to detect in the natural systems (Zark et al., 2015). Alternatively, microorganisms with short generation times, such as *E. huxleyi*, are able to respond to carbonate chemistry alterations through adaptive evolution (Lohbeck et al., 2012) and the magnitude of their physiological responses to acidification differs substantially between strains, since both the adaptation capacity and the sensitivity to environmental perturbations likely have a phenotypic basis (Hoppe et al., 2011). Therefore, we note that more studies should be carried out to define the trends on amount and composition of exudates produced by *E. huxleyi* strains under ocean acidification conditions and their effect on iron biogeochemistry.

## AUTHOR CONTRIBUTIONS

All authors listed have made a substantial, direct and intellectual contribution to the work, and approved it for publication.

## ACKNOWLEDGMENTS

This study received support from the EACFe Project (CTM2014-52342-P) of the Ministerio de Economía y Competitividad of Spain. GS-R. participation was supported by the Grant BES-2011-051448 of the Ministerio de Economía y Competitividad. We thank Dr. Javier Aristegui and the IOCAG for the measurements of dissolved organic carbon, Dr. Manuel A. Coimbra and the QOPNA research unit (University of Aveiro) for the dissolved uronic acids analysis and Judit González for the English revision. We are also grateful to the reviewers for their helpful suggestions.

## SUPPLEMENTARY MATERIAL

The Supplementary Material for this article can be found online at: https://www.frontiersin.org/articles/10.3389/fmars.2018.00210/full#supplementary-material

## REFERENCES

Achterberg, E. P., Holland, T. W., Bowie, A. R., Mantoura, R. F. C., and Worsfold, P. J. (2001). Determination of iron in seawater. *Anal. Chim. Acta* 442, 1–14. doi: 10.1016/S0003-2670(01)01091-1

Allen, A. E., Laroche, J., Maheswari, U., Lommer, M., Schauer, N., Lopez, P. J., et al. (2008). Whole-cell response of the pennate diatom *Phaeodactylum tricornutum* to iron starvation. *Proc. Natl. Acad. Sci. U.S.A.* 105, 10438–10443. doi: 10.1073/pnas.0711370105

Arístegui, J., Duarte, C. M., Reche, I., and Gómez-Pinchetti, J. L. (2014). Krill excretion boosts microbial activity in the Southern Ocean. *PLoS ONE* 9:e89391. doi: 10.1371/journal.pone.0089391

Baldi, F., Marchetto, D., Battistel, D., Daniele, S., Faleri, C., De Castro, C., et al. (2009). Iron-binding characterization and polysaccharide production by *Klebsiella oxytoca* strain isolated from mine acid drainage. *J. Appl. Microbiol.* 107, 1241–1250. doi: 10.1111/j.1365-2672.2009.04302.x

Bastos, R., Coelho, E., and Coimbra, M. A. (2015). Modifications of *Saccharomyces pastorianus* cell wall polysaccharides with brewing process. *Carbohydr. Polym.* 124, 322–330. doi: 10.1016/j.carbpol.2015.02.031

Beaufort, L., Probert, I., de Garidel-Thoron, T., Bendif, E. M., Ruiz-Pino, D., Metzl, N., et al. (2011). Sensitivity of coccolithophores to carbonate chemistry and ocean acidification. *Nature* 476, 80–83. doi: 10.1038/nature10295

Behrenfeld, M. J., and Milligan, A. J. (2013). Photophysiological expressions of iron stress in phytoplankton. *Ann. Rev. Mar. Sci.* 5, 217–246. doi: 10.1146/annurev-marine-121211-172356

Benner, R. (2011). Loose ligands and available iron in the ocean. *Proc. Natl. Acad. Sci. U.S.A.* 108, 893–894. doi: 10.1073/pnas.1018163108

Benson, B. B., and Krause, D. (1984). The concentration and isotopic fractionation of oxygen dissolved in freshwater and seawater in equilibrium with the atmosphere. *Limnol. Oceanogr.* 29, 620–632. doi: 10.4319/lo.1984.29.3.0620

Biddanda, B., and Benner, R. (1997). Carbon, nitrogen, and carbohydrate fluxes during the production of particulate and dissolved organic matter by marine phytoplankton. *Limnol. Oceanogr.* 42, 506–518. doi: 10.4319/lo.1997.42.3.0506

Borchard, C., and Engel, A. (2012). Organic matter exudation by *Emiliania huxleyi* under simulated future ocean conditions. *Biogeosciences* 9, 3405–3423. doi: 10.5194/bg-9-3405-2012

Borchard, C., and Engel, A. (2015). Size-fractionated dissolved primary production and carbohydrate composition of the coccolithophore *Emiliania huxleyi*. *Biogeosciences* 12, 1271–1284. doi: 10.5194/bg-12-1271-2015

Boyd, P. W., and Ellwood, M. J. (2010). The biogeochemical cycle of iron in the ocean. *Nat. Geosci.* 3, 675–682. doi: 10.1038/ngeo964

Boye, M., Nishioka, J., Croot, P., Laan, P., Timmermans, K. R., Strass, V. H., et al. (2010). Significant portion of dissolved organic Fe complexes in fact is Fe colloids. *Mar. Chem.* 122, 20–27. doi: 10.1016/j.marchem.2010.09.001

Boye, M., and van den Berg, C. M. G. (2000). Iron availability and the release of iron-complexing ligands by *Emiliania huxleyi*. *Mar. Chem.* 70, 277–287. doi: 10.1016/S0304-4203(00)00032-3

Breitbarth, E., Bellerby, R. J., Neill, C. C., Ardelan, M. V., Meyerhöfer, M., Zöllner, E., et al. (2009a). Ocean acidification affects iron speciation in seawater. *Biogeosci. Discuss.* 6, 6781–6802. doi: 10.5194/bgd-6-6781-2009

Breitbarth, E., Gelting, J., Walve, J., Hoffmann, L. J., Turner, D. R., Hassellöv, M., et al. (2009b). Dissolved iron (II) in the Baltic Sea surface water and implications for cyanobacterial bloom development. *Biogeosci. Discuss.* 6, 3803–3850. doi: 10.5194/bgd-6-3803-2009

Bundy, R. M., Biller, D. V., Buck, K. N., Bruland, K. W., and Barbeau, K. A. (2014). Distinct pools of dissolved iron-binding ligands in the surface and benthic boundary layer of the California Current. *Limnol. Oceanogr.* 59, 769–787. doi: 10.4319/lo.2014.59.3.0769

Caprara, S., Buck, K. N., Gerringa, L. J. A., Rijkenberg, M. J. A., and Monticelli, D. (2016). A compilation of iron speciation data for open oceanic waters. *Front. Mar. Sci.* 3:221. doi: 10.3389/fmars.2016.00221

Croot, P. L., and Johansson, M. (2000). Determination of iron speciation by cathodic stripping voltammetry in seawater using the competing ligand 2-(2- thiazolylazo)-p-cresol (TAC). *Electroanalysis* 12, 565–576. doi: 10.1002/(SICI)1521-4109(200005)12:8<565::AID-ELAN565>3.0.CO;2-L

Decho, A. W., and Gutierrez, T. (2017). Microbial extracellular polymeric substances (EPSs) in ocean systems. *Front. Microbiol.* 8:922. doi: 10.3389/fmicb.2017.00922

DOE (1994). *Handbook of Methods for the Analysis of the Various Parameters of the Carbon dioxide System in Sea Water,* version 2.1, eds A. G. Dickson and C. Goyet. ORNL/CDIAC-74.

Dupont, C. L., and Ahner, B. A. (2005). Effects of copper, cadmium, and zinc on the production and exudation of thiols by *Emiliania huxleyi*. *Limnol. Oceanogr.* 50, 508–515. doi: 10.4319/lo.2005.50.2.0508

Engel, A., Harlay, J., Piontek, J., and Chou, L. (2012). Contribution of combined carbohydrates to dissolved and particulate organic carbon after the spring bloom in the northern Bay of Biscay (North-Eastern Atlantic Ocean). *Cont. Shelf Res.* 45, 42–53. doi: 10.1016/j.csr.2012.05.016

Engel, A., Thoms, S., Riebesell, U., Rochelle-Newall, E., and Zondervan, I. (2004). Polysaccharide aggregation as a potential sink of marine dissolved organic carbon. *Nature* 428, 929–932. doi: 10.1038/nature02453

Fukuda, S. Y., Suzuki, Y., and Shiraiwa, Y. (2014). Difference in physiological responses of growth, photosynthesis and calcification of the coccolithophore *Emiliania huxleyi* to acidification by acid and $CO_2$ enrichment. *Photosyn. Res.* 121, 299–309. doi: 10.1007/s11120-014-9976-9

Gerringa, L. J. A., Rijkenberg, M. J. A., Bown, J., Margolin, A. R., Laan, P., and de Baar, H. J. W. (2016). Fe-Binding dissolved organic ligands in the oxic and suboxic waters of the Black Sea. *Front. Mar. Sci.* 3:84. doi: 10.3389/fmars.2016.00084

Giuffre, A. J., Hamm, L. M., Han, N., De Yoreo, J. J., and Dove, P. M. (2013). Polysaccharide chemistry regulates kinetics of calcite nucleation through competition of interfacial energies. *Proc. Natl Acad. Sci.* 110, 9261–9266. doi: 10.1073/pnas.1222162110

Gledhill, M., and Buck, K. N. (2012). The organic complexation of iron in the marine environment: a review. *Front. Microbiol.* 3:69. doi: 10.3389/fmicb.2012.00069

Gledhill, M., Achterberg, E. P., Li, K., Mohamed, K. N., and Rijkenberg, M. J. A. (2015). Influence of ocean acidification on the complexation of iron and copper by organic ligands in estuarine waters. *Mar Chem.* 177, 421–433. doi: 10.1016/j.marchem.2015.03.016

González, A. G., Pérez-Almeida, N., Magdalena Santana-Casiano, J., Millero, F. J., and González-Dávila, M. (2016). Redox interactions of Fe and Cu in seawater. *Mar. Chem.* 179, 12–22. doi: 10.1016/j.marchem.2016.01.004

González, A. G., Santana-Casiano, J. M., González-Dávila, M., Pérez-Almeida, N., and Suárez De Tangil, M. (2014). Effect of *Dunaliella tertiolecta* organic exudates on the Fe(II) oxidation kinetics in seawater. *Environ. Sci. Technol.* 48, 7933–7941. doi: 10.1021/es5013092

González-Dávila, M., Santana-Casiano, J. M., and Millero, F. J. (2006). Competition between $O_2$ and $H_2O_2$ in the oxidation of Fe(II) in natural waters. *J. Solut. Chem.* 35, 95–111. doi: 10.1007/s10953-006-8942-3

Gupta, P., and Diwan, B. (2017). Bacterial Exopolysaccharide mediated heavy metal removal: a Review on biosynthesis, mechanism and remediation strategies. *Biotechnol. Rep.* 13, 58–71. doi: 10.1016/j.btre.2016.12.006

Hassler, C. S., Schoemann, V., Nichols, C. M., Butler, E. C. V., and Boyd, P. W. (2011). Saccharides enhance iron bioavailability to Southern Ocean phytoplankton. *Proc. Natl. Acad. Sci. U.S.A.* 108, 1076–1081. doi: 10.1073/pnas.1010963108

Herrero-Martínez, J. M., Sanmartin, M., Rosés, M., Bosch, E., and Ràfols, C. (2005). Determination of dissociation constants of flavonoids by capillary electrophoresis. *Electrophoresis* 26, 1886–1895. doi: 10.1002/elps.200410258

Hider, R. C., and Kong, X. L. (2011). Glutathione: a key component of the cytoplasmic labile iron pool. *Biometals* 24, 1179–1187. doi: 10.1007/s10534-011-9476-8

Hoegh-Guldberg, O., and Poloczanska, E. S. (2017). Editorial: the effect of Climate Change across Ocean Regions. *Front. Mar. Sci.* 4:361. doi: 10.3389/fmars.2017.00361

Hoffmann, L. J., Breitbarth, E., Boyd, P. W., and Hunter, K. A. (2012). Influence of ocean warming and acidification on trace metal biogeochemistry. *Mar. Ecol. Prog. Ser.* 470, 191–205. doi: 10.3354/meps10082

Hogle, S. L., Barbeau, K. A., and Gledhill, M. (2014). Heme in the marine environment: from cells to the iron cycle. *Metallomics* 6, 1107–1120. doi: 10.1039/C4MT00031E

Hoppe, C. J. M., Langer, G., and Rost, B. (2011). Seawater carbonate chemistry and biological processes of *Emiliania huxleyi* (strains RCC1256 and NZEH) during experiments, 2011. Supplement to: Hoppe, C. J. M. et al., (2011): Emiliania huxleyi shows identical responses to elevated pCO2 in TA and DIC manipulations. *J. Exp. Mar. Biol. Ecol.* 406, 54–62. doi: 10.1016/j.jembe.2011.06.008.

Hopwood, M. J., Birchill, A. J., Gledhill, M., Achterberg, E. P., Klar, J. K., and Milne, A. (2017a). A Comparison between four analytical methods for the measurement of Fe(II) at nanomolar concentrations in coastal seawater. *Front. Mar. Sci.* 4:192. doi: 10.3389/fmars.2017.00192

Hopwood, M. J., Rapp, I., Schlosser, C., and Achterberg, E. P. (2017b). Hydrogen peroxide in deep waters from the Mediterranean Sea, South Atlantic and South Pacific Oceans. *Sci. Rep.* 7, 1–10. doi: 10.1038/srep43436

Hudson, R. J. M., Covault, D. T., and Morel, F. M. M. (1992). Investigations of iron coordination and redox reactions in seawater using $^{59}$Fe radiometry and ion-pair solvent extraction of amphiphilic iron complexes. *Mar. Chem.* 38, 209–235. doi: 10.1016/0304-4203(92)90035-9

Hung, C. C., Tang, D., Warnken, K. W., and Santschi, P. H. (2001). Distributions of carbohydrates, including uronic acids, in estuarine waters of Galveston Bay. *Mar. Chem.* 73, 305–318. doi: 10.1016/S0304-4203(00)00114-6

Hurd, C. L., Hepburn, C. D., Currie, K. I., Raven, J. A., and Hunter, K. A. (2009). Testing the effects of Ocean Acidification on algal metabolism: considerations for experimental designs. *J. Phycol.* 45, 1236–1251. doi: 10.1111/j.1529-8817.2009.00768.x

Hutchins, D. A., and Boyd, P. W. (2016). Marine phytoplankton and the changing ocean iron cycle. *Nat. Clim. Change* 6, 1072–1079. doi: 10.1038/nclimate3147

IPCC (2014). *Climate Change 2014:* Synthesis report. Contribution of Working Groups I, II and III to the fifth assessment report of the intergovernmental panel on climate change. In: Pachauri R. K. and Meyer L. A. (ed) IPCC, Geneva.

Jastrzab, R., Nowak, M., Skrobanska, M., and Zabiszak, M. (2016). Complexation copper(II) or magnesium ions with D-glucuronic acid – Potentiometric, spectral and theoretical studies. *J. Coord. Chem.* 69, 2174–2181. doi: 10.1080/00958972.2016.1205738

Jin, P., Wang, T., Liu, N., Dupont, S., Beardall, J., Boyd, P. W., et al. (2015). Ocean acidification increases the accumulation of toxic phenolic compounds across trophic levels. *Nat. Commun.* 6:8714. doi: 10.1038/ncomms9714

Khodse, V. B., Bhosle, N. B., and Matondkar, S. G. P. (2010). Distribution of dissolved carbohydrates and uronic acids in a tropical estuary, India. *J. Earth Syst. Sci.* 119, 519–530. doi: 10.1007/s12040-010-0029-2

King, D. W., and Farlow, R. (2000). Role of carbonate speciation on the oxidation of Fe(II) by $H_2O_2$. *Mar. Chem.* 70, 201–209. doi: 10.1016/S0304-4203(00)00026-8

Kohn, R., and Kovác, P. (1978). Dissociation constants of D-galacturonic and D-glucuronic acid and their O-methyl derivatives. *Chem. Zvesti* 32, 478–485.

Koppenol, W. H., Stanbury, D. M., and Bounds, P. L. (2010). Electrode potentials of partially reduced oxygen species, from dioxygen to water. *Free Radic. Biol. Med.* 49, 317–322. doi: 10.1016/j.freeradbiomed.2010.04.011

Kuma, K., Nakabayashi, S., and Matsunaga, K. (1995). Photoreduction of Fe(III) by hydroxycarboxylic acids in seawater. *Water Res.* 29, 1559–1569. doi: 10.1016/0043-1354(94)00289-J

Laglera, L. M., and van den Berg, C. M. G. (2006). Photochemical oxidation of thiols and copper complexing ligands in estuarine waters. *Mar. Chem.* 101, 130–140. doi: 10.1016/j.marchem.2006.01.006

Lee, R. B. Y., Mavridou, D. A. I., Papadakos, G., McClelland, H. L. O., and Rickaby, R. E. M. (2016). The uronic acid content of coccolith-associated polysaccharides provides insight into coccolithogenesis and past climate. *Nat. Commun.* 7:13144. doi: 10.1038/ncomms13144

Li, F., Pan, B., Zhang, D., Yang, X., Li, H., Liao, S., et al. (2015). Organic matter source and degradation as revealed by molecular biomarkers in agricultural soils of Yuanyang terrace. *Sci. Rep.* 5:11074. doi: 10.1038/srep11074

Lidbury, I., Johnson, V., Hall-Spencer, J. M., Munn, C. B., and Cunliffe, M. (2012). Community-level response of coastal microbial biofilms to ocean acidification in a natural carbon dioxide vent ecosystem. *Mar. Pollut. Bull.* 64, 1063–1066. doi: 10.1016/j.marpolbul.2012.02.011

Lis, H., Shaked, Y., Kranzler, C., Keren, N., and Morel, F. M. M. (2015). Iron bioavailability to phytoplankton: an empirical approach. *ISME J.* 9, 1003–1013. doi: 10.1038/ismej.2014.199

Lohbeck, K. T., Riebesell, U., and Reusch, T. B. H. (2012). Adaptive evolution of a key phytoplankton species to ocean acidification. *Nat. Geosci.* 5, 346–351. doi: 10.1038/ngeo1441

López, A., Rico, M., Santana-Casiano, J. M., González, A. G., and González-Dávila, M. (2015). Phenolic profile of *Dunaliella tertiolecta* growing under high levels of copper and iron. *Environ. Sci. Pollut. Res.* 22, 14820–14828. doi: 10.1007/s11356-015-4717-y

Lu, C.-J., Benner, R., Fichot, C. G., Fukuda, H., Yamashita, Y., and Ogawa, H. (2016). Sources and transformations of dissolved lignin phenols and chromophoric dissolved organic matter in Otsuchi Bay, Japan. *Front. Mar. Sci.* 3:85. doi: 10.3389/fmars.2016.00085

Miller, C. J., Vincent Lee, S. M., Rose, A. L., and Waite, T. D. (2012). Impact of natural organic matter on $H_2O_2$-mediated oxidation of Fe(II) in coastal seawaters. *Environ. Sci. Technol.* 46, 11078–85. doi: 10.1021/es3022792

Miller, W. L., King, D. W., Lin, J., and Kester, D. R. (1995). Photochemical redox cycling of iron in coastal seawater. *Mar. Chem.* 50, 63–77. doi: 10.1016/0304-4203(95)00027-O

Millero, F. J. (1986). The pH of estuarine waters. *Limnol. Oceanogr.* 31, 839–847. doi: 10.4319/lo.1986.31.4.0839

Millero, F. J., Woosley, R., Ditrolio, B., and Waters, J. (2009). Effect of ocean acidification on the speciation of metals in seawater. *Oceanography* 22, 72–85. doi: 10.5670/oceanog.2009.98

Moffett, J. W., and Zika, R. G. (1987). Reaction kinetics of hydrogen peroxide with copper and iron in seawater. *Environ. Sci. Technol.* 21, 804–810. doi: 10.1021/es00162a012

Norman, L., Worms, I. A. M., Angles, E., Bowie, A. R., Nichols, C. M., Ninh Pham, A., et al. (2015). The role of bacterial and algal exopolymeric substances in iron chemistry. *Mar. Chem.* 173, 148–161. doi: 10.1016/j.marchem.2015.03.015

Ozturk, S., Aslim, B., Suludere, Z., and Tan, S. (2014). Metal removal of cyanobacterial exopolysaccharides by uronic acid content and monosaccharide composition. *Carbohydr. Polym.* 101, 265–271. doi: 10.1016/j.carbpol.2013.09.040

Pakulski, J. D., and Benner, R. (1994). Abundance and distribution of carbohydrates in the ocean. *Limnol. Oceanogr.* 39, 930–940. doi: 10.4319/lo.1994.39.4.0930

Papageorgiou, S. K., Kouvelos, E. P., Favvas, E. P., Sapalidis, A. A., Romanos, G. E., and Katsaros, F. K. (2010). Metal-carboxylate interactions in metal-alginate complexes studied with FTIR spectroscopy. *Carbohydr. Res.* 345, 469–473. doi: 10.1016/j.carres.2009.12.010

Passow, U. (2002). Transparent exopolymer particles in aquatic environments. *Prog. Oceanogr.* 55, 287–333. doi: 10.1016/S0079-6611(02)00138-6

Pham, A. N., and Waite, T. D. (2008). Modeling the kinetics of Fe(II) oxidation in the presence of citrate and salicylate in aqueous solutions at pH 6.0–8.0 and 25 °C. *J. Phys. Chem. A* 112, 5395–5405. doi: 10.1021/jp801126p

Piontek, J., Borchard, C., Sperling, M., Schulz, K. G., Riebesell, U., and Engel, A. (2013). Response of bacterioplankton activity in an Arctic fjord system to elevated $pCO_2$: results from a mesocosm perturbation study. *Biogeosciences* 10, 297–314. doi: 10.5194/bg-10-297-2013

Poole, L. B. (2015). The basics thiols and cysteins in redox biology and chemistry. *Free Radic. Biol. Med.* 14, 148–157. doi: 10.1016/j.freeradbiomed.2014.11.013

Price, D., Mantoura, R. F. C., and Worsfold, P. J. (1998). Shipboard determination of hydrogen peroxide in the western Mediterranean sea using flow injection with chemiluminescence detection. *Anal. Chim. Acta* 371, 205–215. doi: 10.1016/S0003-2670(98)00322-5

Pullin, M. J., and Cabaniss, S. E. (2003). The effects of pH, ionic strength, and iron–fulvic acid interactions on the kinetics of non-photochemical iron transformations. I. Iron(II) oxidation and iron(III) colloid formation. *Geochimica et Cosmochimica Acta* 67, 4067–4077. doi: 10.1016/S0016-7037(03)00366-1

R Development Core Team (2013). *R: A language and environment for statistical computing*, Vienna: R Foundation for Statistical Computing. Available online at: http://www.R-project.org/

Read, B. A., Kegel, J., Klute, M. J., Kuo, A., Lefebvre, S. C., Maumus, F., et al. (2013). Pan genome of the phytoplankton Emiliania underpins its global distribution. *Nature* 499, 209–13. doi: 10.1038/nature12221

Rico, M., Santana-Casiano, J. M., González, A. G., González-Dávila, M., and López, A. (2013). Variability of the phenolic profile in the diatom *Phaeodactylum tricornutum* growing under copper and iron stress. *Limnol. Oceanogr.*. 51, 144–152. doi: 10.4319/lo.2013.58.1.0144

Riebesell, U., Schulz, K. G., Bellerby, R. G. J., Botros, M., Fritsche, P., Meyerhöfer, M., et al. (2007). Enhanced biological carbon consumption in a high $CO_2$ ocean. *Nature* 450, 545–548. doi: 10.1038/nature06267

Riebesell, U., Zondervan, I., Rost, B., Tortell, P. D., Zeebe, R. E., and Morel, F. M. (2000). Reduced calcification of marine plankton in response to increased atmospheric $CO_2$. *Nature* 407, 364–367. doi: 10.1038/35030078

Rijkenberg, M. J. A., Gerringa, L. J. A., Carolus, V. E., Velzeboer, I., and de Baar, H. J. W. (2006). Enhancement and inhibition of iron photoreduction by individual ligands in open ocean seawater. *Geochim. Cosmochim. Acta* 70, 2790–2805. doi: 10.1016/j.gca.2006.03.004

Rose, A. L., and Waite, T. D. (2003). Effect of dissolved natural organic matter on the kinetics of ferrous iron oxygenation in seawater. *Environ. Sci. Technol.* 37, 4877–86. doi: 10.1021/es034152g

Roy, E. G., and Wells, M. L. (2011). Evidence for regulation of Fe(II) oxidation by organic complexing ligands in the Eastern Subarctic Pacific. *Mar. Chem.* 127, 115–122. doi: 10.1016/j.marchem.2011.08.006

Roy, E. G., Wells, M. L., and King, D. W. (2008). Persistence of iron(II) in surface waters of the western subarctic Pacific. *Limnol. Oceanogr.* 53, 89–98. doi: 10.4319/lo.2008.53.1.0089

Sachs, J. P., and Kawka, O. E. (2015). The influence of growth rate on $^2H/^1H$ fractionation in continuous cultures of the coccolithophorid *Emiliania huxleyi* and the diatom *Thalassiosira pseudonana*. *PLoS ONE* 10:e0141643. doi: 10.1371/journal.pone.0141643

Samperio-Ramos, G., González-Dávila, M., and Santana-Casiano, J. M. (2018). Impact on the Fe redox cycling of organic ligands released by *Synechococcus* PCC 7002, under different iron fertilization scenarios. Modeling approach. *J. Mar. Syst.* 182, 67–78. doi: 10.1016/j.jmarsys.2018.01.009

Samperio-Ramos, G., Santana Casiano, J. M., and González Dávila, M. (2016). Effect of ocean warming and acidification on the Fe(II) oxidation rate in oligotrophic and eutrophic natural waters. *Biogeochemistry* 128, 19–34. doi: 10.1007/s10533-016-0192-x

Samperio-Ramos, G., Santana-Casiano, J. M., González-Dávila, M., Ferreira, S., and Coimbra, M. A. (2017). Variability in the organic ligands released by *Emiliania huxleyi* under simulated ocean acidification conditions. *AIMS Environ. Sci.* 4, 788–808. doi: 10.3934/environsci.2017.6.788

Santana-Casiano, J. M., González-Dávila, M., González, A. G., Rico, M., López, A., and Martel, A. (2014). Characterization of phenolic exudates from *Phaeodactylum tricornutum* and their effects on the chemistry of Fe(II)-Fe(III). *Mar. Chem.* 158, 10–16. doi: 10.1016/j.marchem.2013.11.001

Santana-Casiano, J. M., González-Dávila, M., and Millero, F. J. (2005). Oxidation of nanomolar levels of Fe(II) with oxygen in natural waters. *Environ. Sci. Technol.* 39, 2073–2079. doi: 10.1021/es049748y

Santana-Casiano, J. M., González-Dávila, M., Rodríguez, M. J., and Millero, F. J. (2000). The effect of organic compounds in the oxidation kinetics of Fe(II). *Mar. Chem.* 70, 211–222. doi: 10.1016/S0304-4203(00)00027-X

Santana-González, C., Santana-Casiano, J. M., González-Dávila, M., and Fraile-Nuez, E. (2017). Emissions of Fe(II) and its kinetic of oxidation at Tagoro submarine volcano, El Hierro. *Mar. Chem.* 195, 129–137. doi: 10.1016/j.marchem.2017.02.001

Shaked, Y., and Lis, H. (2012). Disassembling iron availability to phytoplankton. *Front. Microbiol.* 3, 1–26. doi: 10.3389/fmicb.2012.00123

Shi, D., Xu, Y., Hopkinson, B. M., and Morel, F. M. M. (2010). Effect of ocean acidification on iron availability to marine phytoplankton. *Science* 327, 676–9. doi: 10.1126/science.1183517

Spilling, K., Schulz, K. G., Paul, A. J., Boxhammer, T., Achterberg, E. P., Hornick, T., et al. (2016). Effects of ocean acidification on pelagic carbon fluxes in a mesocosm experiment. *Biogeosciences* 13, 6081–6093. doi: 10.5194/bg-13-6081-2016

Steigenberger, S., Statham, P. J., Volker, C., and Passow, U. (2010). The role of polysaccharides and diatom exudates in the redox cycling of Fe and the photoproduction of hydrogen peroxide in coastal seawaters. *Biogeosciences* 7, 109–119. doi: 10.5194/bg-7-109-2010

Strmečki, S. A., Plavšićc, M., Steigenberger, S., and Passow, U. (2010). Characterization of phytoplankton exudates and carbohydrates in relation to their complexation of copper, cadmium and iron. *Mar. Ecol. Prog. Ser.* 408, 33–46. doi: 10.3354/meps08555

Tagliabue, A., Bowie, A. R., Boyd, P. W., Buck, K. N., Johnson, K. S., and Saito, M. A. (2017). The integral role of iron in ocean biogeochemistry. *Nature* 543, 51–59. doi: 10.1038/nature21058

Tratnyek, P. G., and Hoigné, J. (1994). Kinetics of reactions of chlorine dioxide (OCIO) in water—II. Quantitative structure-activity relationships for phenolic compounds. *Water Res.* 28, 57–66. doi: 10.1016/0043-1354(94)90119-8

Underwood, G. J. C., Aslam, S. N., Michel, C., Niemi, A., Norman, L., Meiners, K. M., et al. (2013). Broad-scale predictability of carbohydrates and exopolymers in Antarctic and Arctic sea ice. *Proc. Natl. Acad. Sci. U.S.A.* 110, 15734–9. doi: 10.1073/pnas.1302870110

Vasconcelos, M. T. S. D., Leal, M. F. C., and van den Berg, C. M. G. (2002). Influence of the nature of the exudates released by different marine algae on the growth, trace metal uptake and exudation of *Emiliania huxleyi* in natural seawater. *Mar. Chem.* 77, 187–210. doi: 10.1016/S0304-4203(01)00087-1

Verdugo, P., Alldredge, A. L., Azam, F., Kirchman, D. L., Passow, U., and Santschi, P. H. (2004). The oceanic gel phase: a bridge in the DOM-POM continuum. *Mar. Chem.* 92, 67–85. doi: 10.1016/j.marchem.2004.06.017

Viollier, E., Inglett, P. W., Hunter, K., Roychoudhury, A, N., and Van Cappellen, P. (2000). The ferrozine method revisited: Fe(II)/Fe(III) determination in natural waters. *Appl. Geochem.* 15, 785–790. doi: 10.1016/S0883-2927(99)00097-9

Wang, Z., and Liu, J. (2014). New insight into photochemical oxidation of Fe(II): the roles of Fe(III) and reactive oxygen species. *Catal. Today* 224, 244–250. doi: 10.1016/j.cattod.2013.09.063

Zark, M., Riebesell, U., and Dittmar, T. (2015). Effects of ocean acidification on marine dissolved organic matter are not detectable over the succession of phytoplankton blooms. *Sci. Adv.* 1:e1500531. doi: 10.1126/sciadv.1500531

**Conflict of Interest Statement:** The authors declare that the research was conducted in the absence of any commercial or financial relationships that could be construed as a potential conflict of interest.